

Appendices

Appendix A

The two Clarke's Orbits Stability and Energy Budget Estimate of Gravitational Sling Shot Model.

In order to determine the stability of the two Clarke's Orbits we will have to analyze total Energy Formulation of a binary system for instance Earth-Moon System and determine its maxima & minima points.

Total Energy of Earth-Moon System = Rotational Kinetic Energy + Potential Energy + Translational Kinetic Energy A.1

Translational Kinetic Energy is of the order of $1 \times 10_{08}$ Joules due to recession of Moon for all practical purposes is negligible as compared to Rotational Kinetic Energy of the order of $1 \times 10_{30}$ Joules. Hence Translational Kinetic Energy is neglected in future analysis.

total energy of the E-M System is:

$$TE = KE + PE$$

Therefore:

$$TE = \frac{1}{2} \times \frac{G(M_{Earth} + M_{Moon})}{a^3} \left[C(E \times a^{1.5} - F \times a^2)^2 + \left(\frac{M_{Moon}}{1 + \frac{M_{Moon}}{M_{Earth}}} \right) a^2 + (0.4 M_{Moon} R_{Moon}^2) \right] - \frac{GM_{Earth} M_{Moon}}{a}$$

Where a=semi-major axis of Moon around Earth;

- $E = 2.13531 \times 10^{-11} \text{ m}^{-3/2}$;
- $F = 9.05036 \times 10^{-16} \text{ m}^{-2}$;
- G = Gravitational Constant;
- C = rotational inertia of Earth around its polar axis;
- M_{Earth} = mass of Earth;
- M_{Moon} = mass of our Moon;
- R_{Moon} = radius of Moon.

To determine the stable and unstable equilibrium points in non-keplerian journey of Moon we must examine the Plot of Eq.A.2 from ' $a' = 8 \times 10^6$ (less than inner Geo-synchronous Orbit radius) to ' $a' = 6 \times 10_{80} \text{ m}$ (greater than outer Ge-Synchronous Orbit).

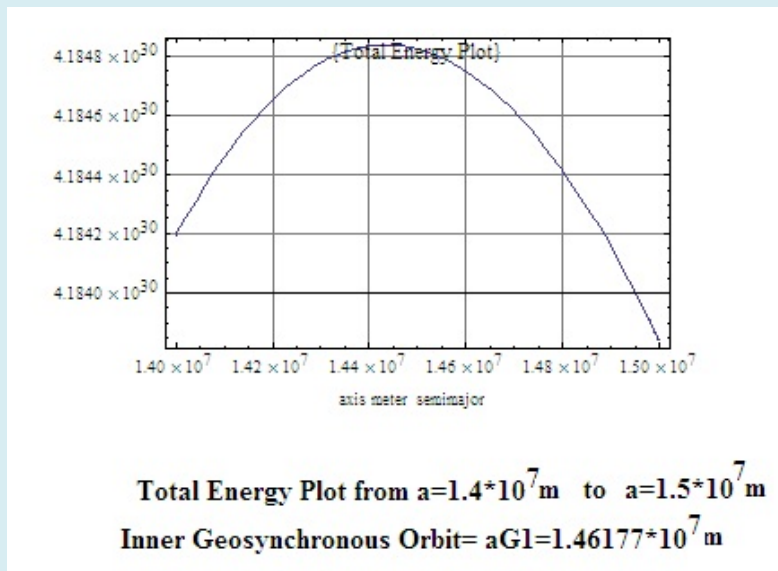


Figure A1: Plot of total energy in the range $1.4 \times 10^7 \text{ m}$ and $1.5 \times 10^7 \text{ m}$ in the vicinity of inner geo-synchronous orbit of $aG1 = 1.46 \times 10^7 \text{ m}$.

We find an energy Maxima at inner geo-synchronous orbit hence it is unstable equilibrium point. When Moon is at inner-geosynchronous orbit, any perturbation launches Moon on either a sub-synchronous orbit or on extra-synchronous (or super-synchronous orbit). If it is launched on sub-synchronous orbit then it rapidly spirals in towards the primary body and if it is launched on extra-synchronous orbit then it spirals out from inner to outer geosynchronous orbit. In our case, Moon is fully formed beyond Roche's Limit which is 18,000Km [84] just beyond inner Clarke's orbit or inner Geo-synchronous Orbit hence Moon is launched on expanding spiral orbit towards outer Clarke's Orbit or outer Geo-synchronous Orbit.

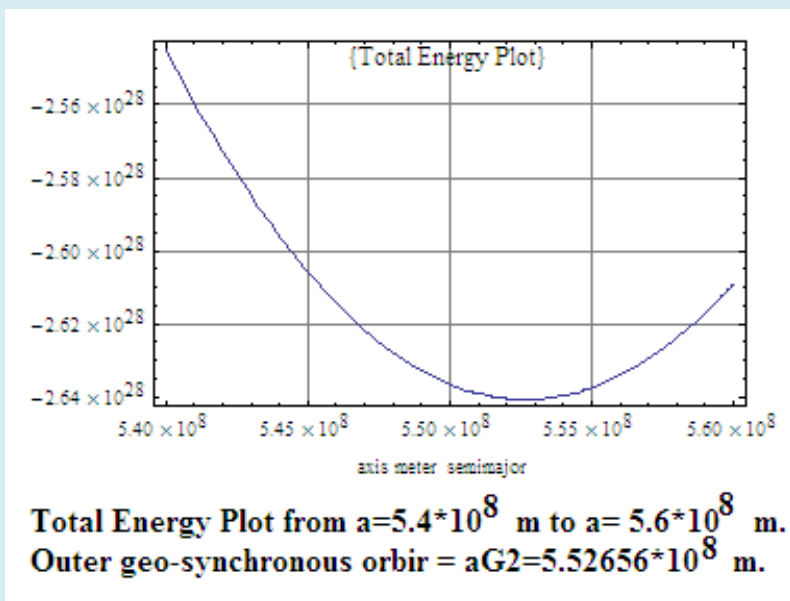


Figure A2: Plot of total energy in the range 5.4×10^8 m and 5.6×10^8 m in the vicinity of the outer geo-synchronous orbit of $a_{G2} = 5.527 \times 10^8$ m.

At outer geosynchronous orbit there is energy minima hence it is stable equilibrium point. Secondary body can never move beyond this orbit. Either it is stay-put in that orbit or it gets deflected back into a contracting spiral orbit.

In a Similar Work by Krasinsky GA [4] the Results Obtained are as Follows:

"Analytical consideration shows that if the contemporary lunar orbit were equatorial the evolution would develop from an unstable geosynchronous orbit of the period 4.42h (in the past) to a stable geosynchronous orbit of the period 44.8 days (in the future). It is also demonstrated that at the contemporary epoch the orbital plane of the fictitious equatorial moon would be unstable in the Liapunov's sense, being asymptotically stable at the earlier stages of the evolution."

In Table A1, a comparison of results of my analysis and that of Krasinsky is given.

	a_{G1}/R_{Earth}	a_{G2}/R_{Earth}	Orbital period at a_{G1}	Orbital period at a_{G2}
Krasinsky analysis	2.15	83.8	4.42h	44.8 days
BKS analysis	2.29	86.65	4.8596h	47.0739 days
Darwin Analysis	Not available	90.4	Not available	47 days

Table A.1: Comparative study of the results obtained by Krasinsky [96], Sharma [95] [personal communication: (2008)]; and Darwin

Energy Budget of Gravitational Sling – Shot Model of Earth-Moon System

The Basic Physics of Gravitational Sling-Shot Model is that when there is considerable differential between Earth's Spin Velocity (ω) and Moon's Orbital Velocity (Ω) there is oscillatory changes in the tidal deformation of Earth and Moon (squeezing and stretching). The tidally deformed shape oscillates between extreme oblateness to extreme prolateness. It is this rapid

oscillation between the two extremes which leads to dissipation of energy and tidal heating because of anelastic nature of Earth. But at the geo-synchronous orbits, a_{G1} and a_{G2} , $\omega = \Omega$ and Earth and Moon are tidally interlocked and during the lock-in stage the two bodies are permanently deformed in oblate shape therefore in these two orbits we have the conservation of energy and the system is a conservative system. At the Mean Motion Resonance (MMR) point $a = a_2$, $\omega/\Omega = 2 = \text{LOM}/\text{LOD}$. In Primary Centric analysis it is assumed that maximum radial velocity (v_{\max}) occurs at $a = a_2$ [3]. After receding to 2:1 MMR point, Moon's recession velocity starts decelerating and today it has decelerated to 3.8cm/yr [30,87,88]. Eventually it will decelerate to 0 cm/yr at a_{G2} .

On the basis of the above reasoning, we have assumed the following: From a_{G1} to a_2 , Earth-Moon System is a conservative system and Moon experiences a powerful sling-shot impulsive torque;

- From a_2 to a_{G2} , Earth-Moon System is a dissipative system;
- From a_{G1} to 0, Earth-Moon System is a dissipative system;
- During the conservative phase from a_{G1} to a_2 when the secondary tumbles in super-synchronous orbit its tidal drag slows down the spin of Earth and pushes out Moon in an expanding spiral orbit as shown Figure 1 of the main Text thereby increasing the orbital period of the Moon and increasing the PE of the E-M system.

At the time Moon is spiraling out three things are happening: The reduction in Earth's spin energy is partially and (reduction in orbital energy fully + reduction in Moon's spin energy fully) are transferred to increase the PE of the system;

- Partially transferred to the translational KE of Moon;
- Remaining is dissipated as heat.

Hence, we can say that between a_{G1} to a_2 : $\{[K \times (\text{reduction in Earth Spin Energy})] + (\text{reduction in orbital energy} + \text{reduction in Moon's spin energy})\}$ – increase in Potential Energy = translational Kinetic Energy in the radial direction.

- Let P1 and P2 be the spin periods of the Earth when the system are in a_{G1} and a_2 configuration.
- At $a_{G1} = 1.46177 \times 10^7 \text{m}$, the Orbital Period of Moon is $P1 = 0.2023 \text{d}$ (4.9hr) by Kepler's Third Law. This is the spin period of Earth also since $\omega/\Omega = 1$.
- At $a_2 = 2.40942 \times 10^7 \text{m}$, the Orbital Period of Moon is $P2^* = 0.4218 \text{d}$ (10.1hr). This is 2:1 Mean Motion Resonance Point where $\omega/\Omega = 2$. Hence Earth's spin is half Orbital Period.

Moon's orbital period increases from 0.2023d (4.9hr) to 0.4218 d (10.1hr). Since a_2 is 2:1 MMR orbit of Moon hence Earth's spin period is half of 0.4218d. Therefore Earth's spin period increases from 0.2023d (4.9hr) to 0.2109d (5.06hr).

Both these slowing down or de-spinning plus the de-spinning of the orbital period lead to increase in the PE of the system and simultaneously imparts the maximum radial velocity to our Moon. It is this recessionary radial Velocity which enables our Moon to coast on its own from a_2 to a_{G2} orbit. At a_{G2} , radial velocity becomes zero and the spiral path terminates at a_{G2} orbital radius. Our Moon will be deflected back into collapsing spiral path due to Sun's tidal interaction [89].

If all the rotational energy given up by Earth and Moon are conserved during conservative phase then: Rotational Energy given up by Earth + Orbital energy given up by E-M system = Increase in PE of E-M System + increase in translational KE of Moon in radial direction. (A.3)

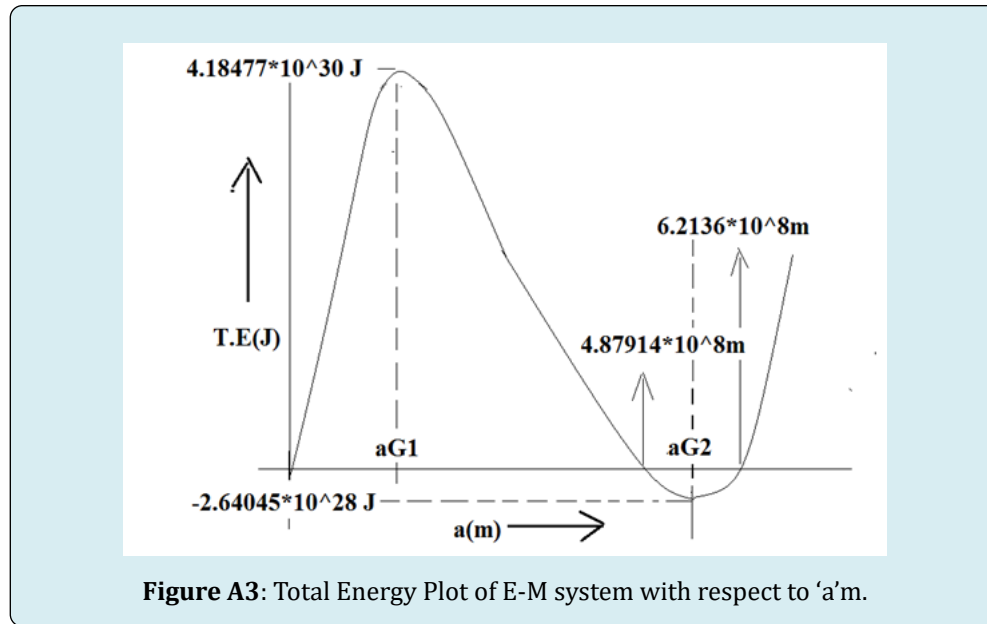
Increase in the PE of E-M system + increase in translational KE in radial direction A.32

Solving Equation (A.3) we get the maximum radial velocity of Moon at $a_2 = v_{\max} = 2115.64 \text{ m/sec}$ which we don't get by Primary-centric analysis. At MMR 2:1 from primary-centric analysis we have $v_{\max} = 1.7178 \text{ m/solar year} = 5.4435 \times 10^{-8} \text{ m/s}$. This means Eq A.3 is not realistic. Even during Sling-shot phase we don't have 100% conservative phase.

Detailed calculation tells us that from a_{G1} to a_2 , 82.7376% of spin and orbital energy given by Earth, Moon and E-M system are transferred to the increase in PE and translational KE and remaining part of the rotational energy is lost as heat. This is expected in the sling shot phase which is relatively conservative.

Detailed calculation also tells us that a_2 to a_{G2} only 12.5% of Earth's spin energy released is transferred to E-M system. 88.5% of energy released goes for tidal heating of our Earth. This is expected in the expanding spiral phase which is dissipative.

By Lunar Laser Ranging present day velocity of recession is 3.8 cm per solar year [30,87,88]



Appendix B

Birth and Evolution of Stars [50,90]

Physics and life cycles of Stars

Mass of the star	Type of Explosion	Mass after the explosion	The process which checkmates the collapse	Type of remnant.
Sun-like	Nova	Less than $1.4M^{\odot}$	Electron degeneracy	White Dwarf
Less than $20 M^{\odot}$	Supernova	$1.4M^{\odot}$ to $3M^{\odot}$	Neutron degeneracy	Neutrinos take away the heat hence a stable Neutron Star is formed with 30km dia.
$20 M^{\odot} > M > 50 M^{\odot}$	Supernova	Greater than $3M^{\odot}$	Quark degeneracy/?	Black hole
$M > 50 M^{\odot}$	Directly collapses into BH	Greater than $3M^{\odot}$	Not Known	Black hole
$M > 140 M^{\odot}$	Pair-instability SN	Not Known	Not Known	No Black Hole

Table B1: The three alternative fates of a star in its death.

Evolution of Stars and Galaxies

- The earliest stars and galaxies were made of pristine materials and they are called Population III stars. They primarily had Hydrogen and Helium with traces of Lithium and Deuterium.
- After the death of Population III stars, heavier elements were introduced through Novae explosions and Super-Novae explosions. Carbon, Neon, Nitrogen, Oxygen, Silicon, Nickel and Iron are introduced in the Universe through Novae explosions. These elements have been nucleosynthesized in the cores of all stars during their Main-Sequence existence.
- Calcium, Magnesium and Titanium and other radioactive elements were synthesized in Super-novae explosions and strewn around the Universe subsequently.
- In 1950, M. Burbidge, G. Burbidge, W. Fowler, F. Hoyle expounded the theory of Nucleosynthesis.

It became clear by theory as well as by careful observations also that as we move from Population III to Population II and now in Population I stars, we find that over time with each successive generation of stars and their novae or supernovae deaths

the gas in galaxies, from which the stars are formed, become enriched in heavy elements. Hence, we conclude that metallicity [% of heavier elements as well as alpha elements abundance = $\alpha/\text{Fe} = (\text{Ca} + \text{Mg} + \text{Ti})/\text{Fe}$] have steadily improved.

Through the study of nearby galaxies, it has been concluded that Milky-way and it's like can retain the enriching products of Supernova explosions and rapidly build up metals and alpha elements in its disk, bulge and halo. This is not the case with nearby Dwarf Galaxies.

Our neighbouring dwarf Galaxies have difficulty retaining gas and products of star formation. This results in large scatter in abundance ratios as well as much slower build-up in alpha elements in Dwarf Galaxies.

We also conclude that the bulk of stellar mass of Population I and II galaxies cannot have come from the merger of two galaxies but that most have come from the gas within the bulge of the galaxy. This means that in first 1 Gy (that is at z , redshift = 5 or larger-see Appendix D) after the Big-Bang according to the current theory of hierarchical structure formation smaller structures (dwarf galaxies) may have merged to form the larger galaxies but in Population I and II smaller galaxies merger is an exception.

The results of the studies conducted by Sloan Digital Sky Survey (SDSS)

Sloan Digital Sky Survey Programme has calibrated the optical spectra of 1 million galaxies in the Local Universe. Most massive galaxies are the oldest, generally elliptical, have very little recent star formation histories and the spectra of the galaxy can be explained in terms of one to three distinct stellar populations namely bulge, disk and halo population.

Typical masses of galaxies have younger average stellar ages, more complicated star formation histories and the overall spectra can be explained in terms of five distinct stellar populations namely extreme disc, thin disc, thick disc, bulge and halo.

This means star formation rate was very high initially and then it monotonically declined. Star formation has in effect moved from most massive galaxies to less massive galaxies.

Here the question arises as to why star formation has stopped in most massive galaxies?

In last twenty years we have built a large number of ground-based giant telescopes of 8 to 10 m diameter. We also have space telescopes such as Hubble Space Telescope, Spitzer Space Telescope and Herschel Space Observatory. Study of young massive stars provide the most useful tracers of star formation activity as enumerated in Table B3.

Tracer number	1	2	3	4
Property of the tracer	Bright optical-UV continuous light from star themselves	Bright H2 & O2 emission lines from the surrounding gas ionized by the hot stars	Enhanced emission at Mid & Far infra-Red from the dust warmed by UV light from the stars.	Radio-emission from the relativistic electrons accelerated by the shock waves produced by Supernova explosions.

Table B.3: The useful tracers of star formation activity in Young Massive Stars.

Star Formation Rate through the cosmic times [91,92]

After extensive studies particularly those of Sloan Digital Sky Survey (SDSS) we have arrived at the Figure B.1 and concluded the following results in Table B4

Time after BB	Z_{\uparrow} (redshift) Or T(Kelvin)	Event	Comment
0 year	Infinite	Big Bang occurs	Time is born with Big Bang
10^{-43}s	$3.16 \times 10^{31}\text{K}$	1st Symmetry breaking	Quantum Gravitation to GUT phase transition.
			Relic gravitons left out.
			Density of matter = 10^{93}gms/cc .

10^{-10} s	10^{15} K, 100GeV	2nd Symmetry breaking	GUT to Electro-Weak Phase transition, weak force decouples, relic intermediate vector bosons left out, Universe filled with a soup of quarks, leptons, photons
10^{-6} s	10^{13} K, Less than 1GeV	Fission of nuclear particle stops	Quark-nucleon phase transition. Universe filled with a soup of leptons, nucleons, photons.
			Relic quarks left out.
			Density of matter = 10^{18} gms/cc.
10^{-4} s	10^{12} K; 1000×the core temp of Sun	Instability of leptons lead to instability of baryons.	Continuous transmutation taking place between proton and neutron. Density of matter = 10^{14} gms/cc.(nuclear density)
4sec	5×10^9 K	Leptons become stable hence baryons stabilize.	p, n stabilizes to 7:1
3min	745×10^6 K		75%H ions, 25% He ions
15mins	333.3×10^6 K	Nuclear fusion first stage completed.	Matter in plasma form stabilized at 75%H ions, 25% He ions or 92% and 8% by atomic number density with traces of Lithium
From here onward Universe enters the Dark Ages. But the matter is not uniformly distributed as confirmed by the study of Cosmic Microwave Background Radiation through COBE and WAMP. The denser part of matter shows up as red in CMBR map and rarefied part shows up as blue. The denser part are the seeds of stars, galaxies and clusters. CMBR carries the imprint of the matter distribution at the time of decoupling which will occur at 380,000 years after the BB because temperature cools below 4000K which allows plasma to neutralize.			
380,000yrs	4000K	Plasma recombines into cold, neutral, dark universe.	Temperature of the Universe falls to 4000K where all ions recombine to form neutral atoms and molecules of H ₂ and He. Gravity will dominate from now on.
The stage is set for the formation of Population III stars and galaxies.			
500My	Z=8.5	Not Known	Not Known
600My	Z=7	Dark age ends and the epoch of reionization begins	Population III stars and galaxies are formed and these re-ionize the cold, neutral and dark universe. (detected by near-IR Wide Field Camera3 mounted on Hubble Space Telescope).
Population III stars were massive and hence short lived however through internal fusion followed by supernova explosion they must have commenced the process of chemical enrichment through recycling in the interstellar matter. This produced the successive generations of Population II and Population I stars with progressively higher metallicity and alpha elements.			
1Gy	Z=6	Rapid build-up of low metallicity stars.	Here heavier elements reside in cool gas and dust grains within the Galaxies.
2Gy	Z=3	Metallicity increases through nuclear synthesis. Star formation Rate = $\rho = 0.2^*$	Heavier elements reside in stars, planets and interstellar gas. There is possibly a peak in Star Formation Rate.
3Gy	Z=2	Half the stars were in place and $\rho \geq 10 \rho_0$	Population II & Population I stars and Galaxies are born. Milky Way is born at this time. It is the third Generation Galaxy (Population I).
4Gy	Z=1	Rate of star formation is $10 \rho_0 = 0.1^*$	
9.133Gy		Our Solar Nebula is born.	Our Sun is Population I star.

13.7Gy (present)	$Z=0$	Rate of star formation is $\rho_0=0.01^*$	
---------------------	-------	--	--

Table B4: The Cosmic History of Star formation.

*Units of star formation rate is (MSUN) $\times y^{-1} \times \text{Mpc}^{-3}$, ρ_0 = present day star formation rate;

†Distance calculation from Redshift (z) is given in the Appendix D.

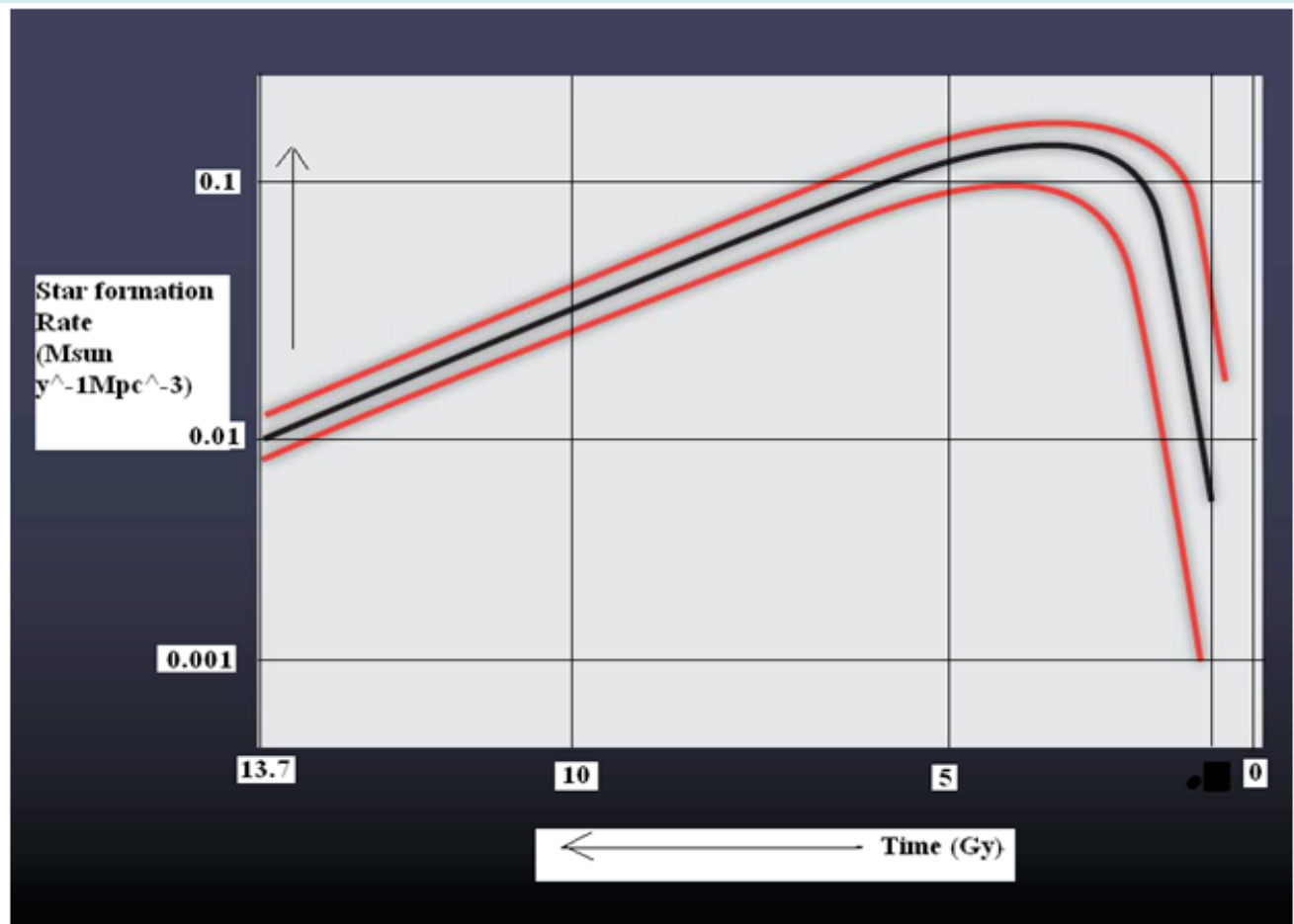


Figure B1: A simple representation of our current knowledge of the rise and fall of globally averaged star-formation activity over the 13.7 billion years of cosmic history. The black line indicates our best estimate of how the density of star formation (in solar masses formed per year per unit of co-moving volume) grew rapidly in the first 2 billion years after the Big Bang, stayed roughly constant for a further ~ 2.5 billion years, then has declined almost linearly with time since the universe was ~ 5 billion years old. The red lines indicate the typical current uncertainty in the measurement, which rises to approximately an order of magnitude at the earliest times.

Appendix C

Formation and Evolution of Galaxies [44,64]: Through the advancement of γ -Ray and X-Ray astronomy it has been possible to peer into the nuclei of several galaxies and through the study of the last decade it is confirmed that probably all the Galaxies have Super Massive Black Holes (SMBH). It is confirmed that the lives of Galaxies and MBHs are inextricably intertwined. It can also be said that as the galaxies grow so do the MBH at the center.

Quantum Mechanical fluctuations in the Universe emerging from the Big Bang gave rise to the small inhomogenities which will act as the future seeds of the super clusters, cluster and galaxies. These inhomogenities attracted the surrounding matter gravitationally and grew into lumps called haloes. In these haloes there is gravitational heating as we see in Pre-Main

Sequence Stars and there is radiative expansion and cooling. The two are trying to compensate each other. If gravitational heating dominates there will be subdued star formation and if radiative cooling takes place then there will be rapid star formation.

In low-mass haloes below critical mass $10^{12} M_{\odot}$, cooling dominates and there is a star formation burst due to cold gas inflow. This is how the spiral galaxies grow by gas accretion.

In high-mass haloes above $10^{12} M_{\odot}$, heating dominates and growth stops by accretion. Halo mergers take place leading to large haloes. Within the large haloes galaxy mergers take place and spiral galaxies disks are scrambled into bulgy elliptical galaxies.

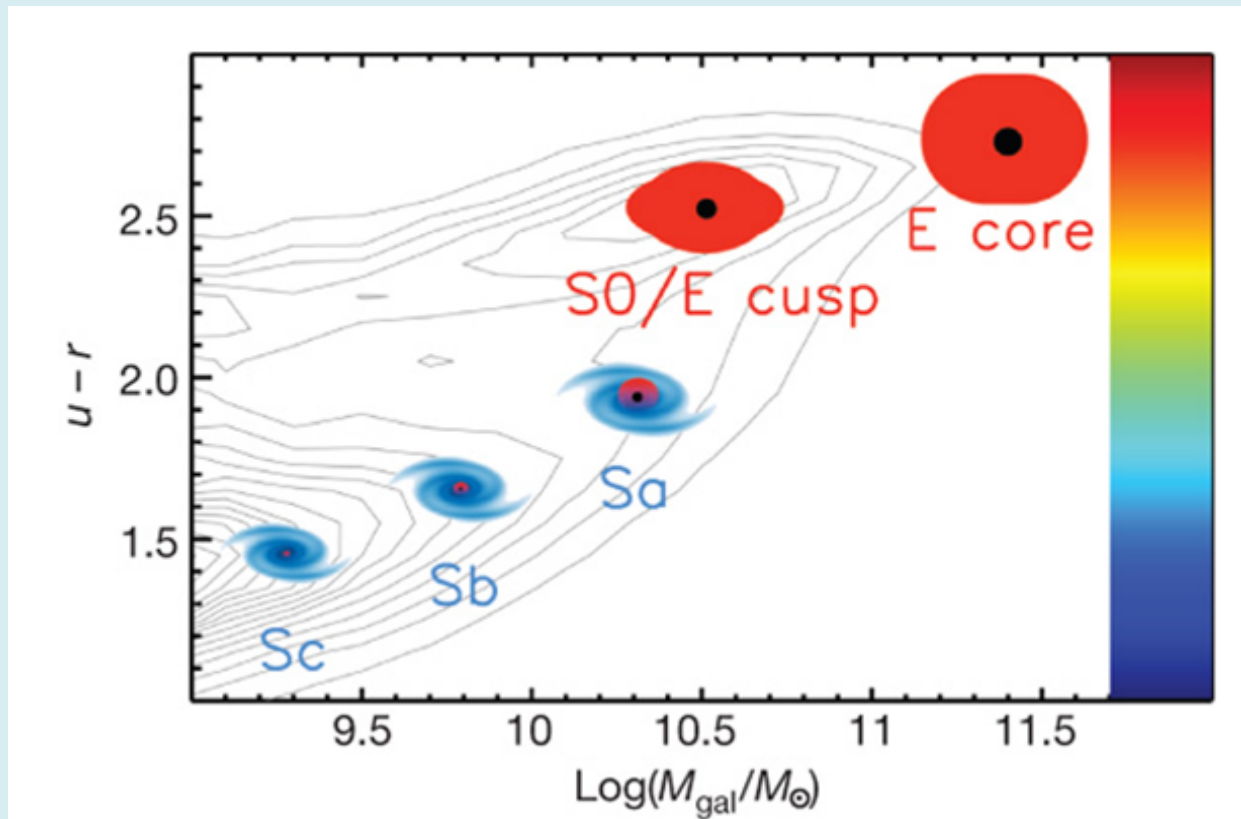


Figure C1: The contours show the galaxy distribution on a stellar mass (M_{gal}) – colour diagram. The difference between ultraviolet luminosity and red luminosity, quantified by the magnitude difference $u - r$, is a colour indicator; larger values of $u - r$ correspond to redder galaxies. The colour bar has been inserted to convey this notion visually and has no quantitative meaning. Galaxies are classified into two main types: spirals that mainly grew through gas accretion ('S', shown in blue) and ellipticals that mainly grew through mergers with other galaxies ('E', shown in red). 'S0' galaxies are an intermediate type, but we assimilate them to ellipticals. Spirals have central bulges, shown in red, that resemble miniature ellipticals. All ellipticals and bulges within spirals contain a central black hole, shown with a black dot. Moreover, ellipticals and bulges within spirals have the same black-hole mass to stellar mass ratio, of the order of 0.1%. This is why we call them 'bulges' indiscriminately. In contrast, there is no connection between masses of black holes and masses of disks (the galactic component shown in blue). Spirals and ellipticals are separated by a colour watershed at $u - r \approx 2$ and a mass watershed at $M_{\text{gal}} \approx M^* \approx 10^{10.5} M_{\odot}$. M^* is of the order of $\text{fb} M_{\text{crit}}$, where $M_{\text{crit}} 10^{12} M_{\odot}$ is the critical halo mass for gas accretion and $\text{fb} 0.17$ is the cosmic baryon fraction. Spirals form a sequence where the bulge-to-disk ratio tends to grow with M_{gal} (Sc, Sb, Sa). Ellipticals have two subtypes: giant ellipticals with smooth low-density central cores formed in mergers of galaxies that have long finished their gas ('E core') and lower-mass ellipticals with steep central light cusps formed in mergers of galaxies that still have gas ('E cusp'). Whereas core ellipticals formed all their stars over a short time span at high redshift, the formation of the lower-mass cuspy ellipticals from the 'quenching' and reddening of blue galaxies continues to low redshift [This Figure is from Ref 43 in the main Text.]

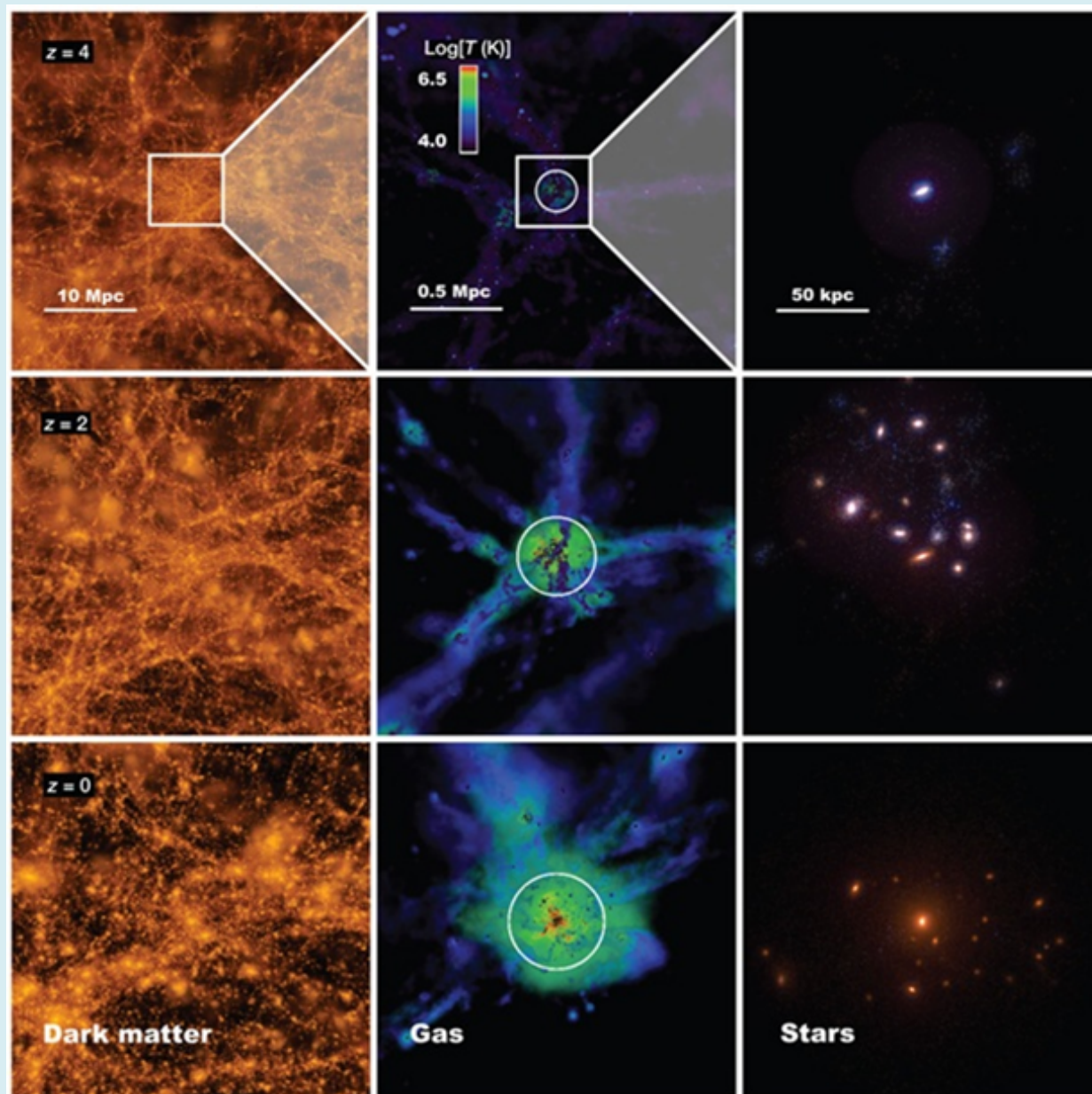


Figure C2: A computer simulation of the formation of an elliptical galaxy. The nine panels illustrate the formation of an elliptical galaxy by showing how the dark matter (left column), the gas (centre column) and the stars (right column) are distributed at three epochs in the expansion of the Universe: when the Universe was 1/5 of its current size (redshift $z = 4$), when the Universe was 1/3 of its current size ($z = 2$), and today ($z = 0$). The gravity of the dark matter dominates the evolution on large scales (left column). As time passes, the Universe becomes lumpier because the dark matter clumps via gravity into haloes (bright orange spots in the left panels). The centre column zooms into the region around and inside a halo to show what happens to the gas. The halo radius is shown as a white circle, and the gas is colour-coded according to its temperature: blue is cold, green (and red) is hot. Initially the halo is small, and the gas streams into the halo down to its centre in cold flows. When the halo reaches the critical mass $M_{\text{crit}} = 10^{12}$ ($z = 2$), the gas begins to form a hot atmosphere (green); eventually, all the gas within the halo is hot ($z = 0$). The right column zooms in even further to show the visible galaxy formed by the gas fallen to the centre. The galaxy is initially a blue spiral ($z = 4$). It starts to become red when the halo gas starts to be hot ($z = 2$). By then, its halo has merged with neighbouring haloes to form a galaxy group. Mergers with companions eventually transform the galaxy into an elliptical ($z = 0$) [This Figure is from Ref 43 in the main Text].

Most MBHs are turned off or dormant. But if there is a disc of accretion, the gas and dust within the radius of influence will be sucked into the BH just as a vortex in a river sucks in the surrounding water. When the reservoir of gas and dust is exhausted this accretion will stop and BH will shut-off.

In-falling gas and dust emits radiation in γ_{ray} , X-Ray, Ultra-Violet and optical part of the spectrum. These AGN are seyfert galaxies [79].

Apart from these emissions there are conical relativistic jets being emanated from the poles of the BH [93]. Unsteady accretion flow gives rise to variable AGN. The most variable AGN are a sub-class called Blazars with typical masses of 10^8 to 10^9 M_{\odot} . It is radio and optically bright, but luminosity is dominated by X-ray and γ -ray. Doppler beam emitting region within a jetted outflow moving relativistically causes changes on minutes- to hours- time scale. The high energy emission is caused by Inverse Compton Up-Scattering of accretion disk photons. The conical emanation takes place in Super Massive Black Hole engulfing a large amount of surrounding gas and dust [94-97]. The same kind of jets can be emanated from Massive Black Hole which is tidally shredding the star launched on a death spiral towards the nucleus of the Galaxy [21,22]. The two conical jets are very narrow streams of particles travelling in opposite directions at relativistic speeds. These relativistic jets travel out to distances across the Galaxy.

As they emerge out of the two poles of the galaxy they finally decelerate as they interact with the interstellar gas and dust, and they turn on two radio-emitting lobes. This kind of Active Galactic Nucleus (AGN) is called QUASERS as shown in the Figure C3.



Figure C3: Twin jets produced by the supermassive black hole in the galaxy Messier 84 are strongly interacting with the hot tenuous gas in the galaxy's halo. The black hole is located at the center of the brightest region in this image. The jets are traced by their radio emission (shown in red) as mapped with the Very Large Array (VLA), and the hot gas is traced by its x-ray emission (shown in blue), as mapped with the Chandra X-ray Observatory. The jets decelerate as they travel out into the halo and light up as two lobes of radio emission. These lobes form two cavities in the hot gas as they push it out of their way. [Source: x-ray, NASA/Chandra X-ray Center (CXC)/Max Planck Institute for Extraterrestrial Physics/A. Finoguenov; radio, NSF/National Radio Astronomy Observatory/VLA/European Southern Observatory/R. A. Laing; optical, Sloan Digital Sky Survey].

The Star population converts 0.7% of Solar Nebular Matter into energy by nuclear reaction from which it has been born. In contrast SMBH in AGN accretes 10% of the rest mass in the bulge of the Galaxy and converts it into energy. Hence, they (AGN) stand out as distinct cosmic beacons clear across the Universe. Through such beacons, distance estimate can be made for the far-flung Galaxies. Detection of GRB090429B, the most distant GRB (Gamma Ray Burst), is a case in point [98] and these beacons will also let me know how the SMBH have evolved across the entire span of cosmic time. We have different categories of AGN and accordingly we have different categories of Galaxies such as Seyfert Galaxies, Blazars and QUASERS. All these three play an important role in anchoring Clusters and Super-Clusters.

Even a tiny fraction of ($<1\%$) of this energy released within each bulge could heat and blow away the entire gas content from the bulge and completely stop star formation.

The results of Galaxy Classification by Galaxy Zoo [99].

Galaxy Zoo was an online classification program for all the galaxies catalogued by Sloan Digital Sky Survey (SDSS) over a period of 11 years. The results have been tabulated in Table (C1).

	Blue (indicative of star formation)	Red (star formation quenched)	
Spiral Galaxy	80% Here gas component is large hence star formation is high.	20%_these are barred red spirals. Hydrogen is being siphoned off from the halo and star formation is retarded	
Elliptical Galaxy	20%_these are recently formed small galaxies and are undergoing vigorous star formation.	80% These lack gas hence star formation has stopped. Only old light mass stars are there	
Little Green Galaxies			Compact galaxies. These undergo extreme star formation and emit light at a wavelength that is characteristic of highly ionized oxygen. In SDSS images these appear green.

Table C1: Classification of Galaxies based on the Galaxy Zoo program.

Astronomers have concluded that galaxies are formed when dark matter clusters together under its own gravity and then pulls gas, dust, stars and smaller galaxies to form the flat extended disk of a spiral galaxy. Dark matter stays in the spherical “halo” that surrounds the whole galaxy. In spiral galaxies, stars keep forming in the disk as neutral gas rains down from halo into the spiral arms.

Elliptical galaxies result when two galaxies of comparable masses collide- if one or both are spiral galaxies, the spiral structure is destroyed, and stars are left in random orbit around the galactic center. The collision also slams together gas clouds causing burst of intense star formation that flares and burns out quickly using up all the hydrogen gas. The end result is a structure less blob of a galaxy with no gas clouds and few young stars.

Galaxies grow by accretion of surrounding cool gas in the halo or the merger between two or more galaxies. This merger takes place in seven distinct steps:

- Two galaxies merge together as shown in Figure E.11, Appendix E. Thin and highly ordered disk components are scrambled together.
- Tidal forces between the two galaxies drain away angular momentum from the cold gas in the disk of the galaxy, allows the cold gas to flow into the inner region and then fuels an intense burst of star formation. This flow delivers a fresh supply of gas to SMBH as shown in Figure E.12..
- The scrambled disk material settles into a newly created bulge.
- If the two progenitors had their own BH then the two also merge to give rise to a new BH as shown in Figure F.13.
- The release of energy from the merger induces a star formation burst so intense that it may blow away most or all remaining gas in a powerful outflow.

- Relativistic conical jets from SMBH will pump energy into the surrounding gas preventing it from cooling and falling into the galaxy thus quenching star formation.
- Finally we have a single Galaxy with a larger bulge and a larger SMBH as shown in Figure E.13.
- Living Galaxy has reached its limit of growth and it becomes passive. Star formation stops. BH growth also stops.

Growth rate of Galaxies and SMBH depend strongly on mass [100]. As we see in Figure E17, in Appendix E, most massive galaxies and their respective SMBHs grew rapidly early in the cosmic history and then they stopped growing after reaching a limit. In contrast as seen in Figure E.18, lower mass galaxies and their respective BHs have grown at a lower uniform rate throughout the entire cosmic history.

Apart from these major mergers there are minor mergers. Our Milky Way has assembled itself from a kit of hundred of Galactic building blocks. Whenever a small galaxy or a star cluster passes by too close, our Galaxy's gravity tears it apart and draws it into the main galaxy [61,63]. Our Milky Way's, and so Galaxy's in general, tangled history of merging and accreting have brought new stars, gas and dark matter within the halo of our Milky Way. In fact merger and accretion are processes which have become the main driver of Galaxy formation and evolution. These minor mergers have also revealed the nature of dark matter- its hydro-static equilibrium shape and its granularity.

Different classes of Galaxies according to the mass of BH [44]

Mass of BH	Accretion disc	Spin Rotation	Spectrum	Name of the galaxy
$10M^{\odot}$		Not Known	Not Known	This is not the fulcrum of the galaxy and is the result of the death of a massive star of mass $> 20M^{\odot}$
10^5 to 10^6M^{\odot} (moderateBH)	No	Little or no	quiet	Fulcrum of light weight Galaxy
10^5 to 10^6M^{\odot} (moderateBH)	Yes	Yes	IR to γ -Ray continuous	Fulcrum of Seyfert galaxy.
10^6 to 10^8M^{\odot} (MBH)	Yes. Rate of BH growth/ $\rho_{\text{SFR}}^* = 0.7361111111111111$	Yes	More luminous and radio loud.	Fulcrum of Intermediate galaxies.
10^8 to $10^{10}M^{\odot}$ (SMBH)	No Lack cold, dense gas.	Not Known	Switched off	Fulcrum of massive galaxies. Buried in aged Galaxies with little or no reservoir of cold, dense gas.
10^8 to $10^{10}M^{\odot}$ (SMBH)	Mass ratio of SMBH/Mass of the bulge = 1:1000, Surrounded by a halo of hot and tenuous gas		Switched on.	Fulcrum of massive galaxies. Active Galactic Nuclei (AGN) †. It has relativistic jet and strong emissions. It heats the surrounding gas. This shuts off the star formation

Table C2: Classification of Galaxies according to the mass of the BH.

* ρ_{SFR} = star formation rate. †AGN can be a sub-class of Blazer or it can be QUASER.

There is a strong connection between Star Formation Rate (ρ_{SFR}) in the bulge and the growth rate of SMBH. When there is a sufficiently large reservoir of cold, dense gas then both processes are supported.

The self-regulating process which keeps Mass ratio of (SMBH/Mass of the bulge) = 1:1000 or which keeps Rate of BH growth/ $\rho_{\text{SFR}} = 1:1000$ is by feedback mechanism as given below:

- In Galaxies hosting 10^8 to $10^{10}M^{\odot}$ (SMBH), powerful relativistic conical jets are created which prevent the in-fall of cool gas into the bulge. Hence star formation is quenched and growth of SMBH is stopped.

- In intermediate mass Galaxies hosting 10^6 to $10^8 M^\odot$ (MBH), SN explosions due to the death of newly formed massive stars causes an out-flowing galactic wind. This sweeps away Galactic gas into the halo where it is in hot form. This also regulates the availability of cool gas in the bulge thereby regulating the star formation rate and growth rate of MBH to the ratio 1000:1.

In a living galaxy or young galaxy, stars formation is going on and accretion of gas and dust on the BH is also going on. The accretion by BH leads to Gamma Ray Burst (GRB) and relativistic Jets. Gamma Ray Bursts are the Universe's most luminous explosions emitting more energy in a few seconds than our Sun will during its energy producing life-time.

Massive stars collapse into Black Holes surrounded by a dense hot disk of gas. The in-falling matter is diverted into a pair of high energy jet particles that tear through the collapsing star. The jets move upward at 99.9% of the speed of light. The jet of particles strikes the gas beyond the star to produce afterglows. "Catching these afterglows before they fade is the key to determine the distances of the bursts."

GRB090429B has qualified as the most distant galaxy till date [98]. It was detected by its Gamma Ray Burst. It is at 13.14 billion light years distance with date of occurrence at 520My after the Big Bang when the Universe was 4% of the present age and 10% of the present size. This is the first galaxy to form after the Big Bang.

James Well Space Telescope due to launch in 2017 has been carefully engineered for studies in the early Universe. An after-glow spectrum from this facility would be an unique and valuable source of data.

Penn State University, Southwest Research Institute, Cornell University have proposed JANUS explorer to be launched by 2017. This will be used for understanding the first galaxies and the various processes guiding their formation.

By discovering and observing the most distant GRBs and QUASERS and measuring their distances autonomously without the need for follow up observation, JANUS would provide a steady stream of rewarding targets to James Well Space Telescope and ground-based telescopes.

Nothing else illuminates the conditions in the early Universe like the brightest lights of GRB and QUASERS.

Massive stars are dying, leading to SN explosions. The strong emissions from SN explosions and relativistic jets are heating up the gas in the halo and SN explosions are powering an outward galactic wind that can sweep out the Galaxy's gas and sweep it into the halo. For a given black hole mass, there is a maximum AGN luminosity, called the Eddington limit, above which the radiation-pressure force outwards exceeds the gravitational force inwards, suppressing the gas flow onto the black hole. The velocity dispersion is the bulge property that is most closely linked to the black hole because it determines the depth of the potential well from which the gas has to be expelled, and thus the minimum black hole mass for feedback. At the Eddington Limit, star formation is halted as well as the growth of black hole is stopped, and Galaxy is switched off. Young and living Galaxy is turned into aged and passive galaxy. This self-regulating process has kept the mass ratio pinned down to 1:1000 in the early galaxies and keeps Rate of BH growth/ $\rho_{\text{SFR}} = 1:1000$ in the present-day galaxies.

There is always fresh cool and dense gas coming in the bulge from the outer disk subsequently. There is also the remnants of the dying stars being fed into the bulge. Both these factors eventually may rejuvenate the dormant galaxy.

90%	No conical jet of energetic particles	
10%	Have conical jet	Radio Galaxies, Quasars and Blazers

Table C3: Classification of AGN.

- Different orientation of observation also gives rise to different galaxies.
- If we look down the conical barrel of emission then we have Quasars and Blazers,
- If we look broadside, then we have Seyferts Galaxies.

	Nucleus brightness variation time scale	Spectrum	At the nucleus	Total luminosity
Seyferts Appendix E. Figure E.14	Months	Continuous, absorption lines, strong emission lines of H and also of O	Shoot out narrow beams of energetic electrons producing synchrotron radiation.	$10^{10}L_0$
QUASER Figure C.3	X-ray variation in days, hours, mins	Continuous, absorption lines, strong emission lines of H and also of O	It outshines the stars. It has relativistic conical jets and two radio lobes	$10^{12}L_0$
Blazers Appendix E. Figure E.15	Optical vari. Over days.	High radio brightness, high optical polarization; Widest range of frequencies from radio to γ -Ray.	It has relativistic jets pointed to Earth	

Table C4: Classification of Seyferts, QUASERS and Blazers.

Two sub-groups of Blazers:

- Sources showing strong and broad emission lines, such as those of quasars (called Flat Spectrum Radio Quasars)
- Sources showing a featureless optical spectrum (called BL Lac objects) [101] [Urry (1998)].

Appendix D

Galactic distances are measured using the Hubble relationship:

$$v = Hd \text{ (D1)}$$

where $H = 71 \text{ Km}/(\text{sec.Mpc})$ [7-year release in 2010 from WMAP data alone]

and $1 \text{ Mpc} = 3.26 \text{ ly}$ (light-year).

- Velocity of recession has to be determined from Z (red shift).
- Z (Doppler shift) has to be determined by spectroscopy.
- Observed Wavelength (λ_{OBS}) are determined by observation and Emitted Wavelength (λ_{EMITTED}) are determined by spectroscopy science.

$$(\lambda_{\text{OBS}}) = (\lambda_{\text{EMITTED}}) \times (1 + z) \quad (\text{D2})$$

$$Z(\text{red shift}) = \Delta\lambda / \lambda = (\lambda_{\text{OBS}} - \lambda_{\text{EMITTED}}) / (\lambda_{\text{EMITTED}}) = (1 + v/c) / \sqrt{1 - v^2/c^2} - 1 \quad (\text{D3})$$

From Eq.D.3, velocity of recession of the given Galaxy is determined.

Receding galaxies spectrum suffer from Doppler Red Shift.

Velocity of recession gives distance in light-years using Hubble relationship Eq. D1.

Vreca(m/s)	Z shift	d(ly)
1×10^8	0.414	4.591G
1.5×10^8	0.732	6.887G
2×10^8	1.2361	9.183G
2.5×10^8	2.3166	11.478G
2.7×10^8	3.3589	12.397G
2.8×10^8	4.3852	12.856G
2.9×10^8	6.68	13.3G
2.95×10^8	9.91	13.545G
2.99×10^8	23.47	13.728G

Table D1: Distance of Galaxies and QSO (quasi stellar objects) based on Z measurement.

Appendix E

Extension of the New Perspective as the principal formative process in shaping the Universe - GRB110328 comes as a grand vindication of the New Perspective based on Gravitational Sling-Shot Model of Earth-Moon System [21,22].

A long duration Gamma Ray Burst (GRB110328) was picked up by Burst Alert Telescope (BAT) aboard SWIFT Gamma Burst Mission Spacecraft. Emission of X-Rays and Gamma Ray is persisting. It seems a Super Massive Black Hole (SMBH) situated at the centre of a Galaxy 3.8 billion light years away with a red-shift of 0.3534 was ripping apart a star of about sun's mass (M_{\odot}) and SMBH was gobbling it up gradually. It was the biggest and the brightest event in the series of GRB and QUASERS observed till now. Earth was in line with the Jet emission. SWIFT was looking down the conical barrel of X-Rays and γ -Rays. This conical barrel is normal to the plane of the star's orbit of death spiral. This event was reported by Bloom JS of University of California and by Andrew Levin et al of University of Warwick in 8th July 2011 Science Vol 333.

This long duration GRB may not be rare but SWIFT falling in line of sight of the conical barrel of this stupendous emission is a very rare event. This happens 1-in- $10_8 \sim 10_9$ events.

Gamma-ray bursts (GRBs) are the most powerful explosions the Universe has seen since the Big Bang. They occur approximately once per day and are brief, but intense, flashes of gamma radiation. They come from all different directions of the sky and last from a few milliseconds to a few hundred seconds. So far scientists do not know what causes them. Do they signal the birth of a black hole in a massive stellar explosion? Are they the product of the collision of two neutron stars? Or is it some other exotic phenomenon that causes these bursts?

With SWIFT, a NASA mission with international participation, scientists have a tool dedicated to answering these questions and solving the gamma-ray burst mystery. Its three instruments give scientists the ability to scrutinize gamma-ray bursts like never before. It has three instruments aboard: 1.BAT-Burst Alert Telescope; 2.XRT-X-Ray Telescope; 3.UVOT-Ultraviolet/Optical Telescope. BAT scans 1/6 of the sky at one time. Within seconds of detecting a burst, it directs XRT and UVOT to lock on the GRB and study the afterglow in X-Ray, UV and Visible range of the electromagnetic spectrum. Swift relays its location to ground stations, allowing both ground-based and space-based telescopes around the world the opportunity to observe the burst's afterglow. Swift is part of NASA's medium explorer (MIDEX) program and was launched into a low-Earth orbit on a Delta 7320 rocket on November 20, 2004.

With better luck, or more advanced facilities, it should be possible in the future to use the bright afterglows of bursts like GRB 090423 and GRB 090429B to explore the conditions of star and galaxy formation at these early cosmic epochs in detail. "Discovering extremely distant bursts is pretty fun," says Fox, "but we suspect there is a whole lot more information in the bursts, waiting for us, that we have yet to access."

GRB as indicated by the above two events are extremely bright and these are detectable at long distances. GRB090423 spectra gave a red-shift of $z=8.2$ indicative of 13.04 billion light years distance and GRB090429B gave a red shift of $z=9.4$ indicative of 13.14 billion light years. Gamma Ray Burst is short lived event lasting less than 10 seconds. They have a faint after-glow in X-Ray region and in IR region but give no glow in optical region. Visible region "Drop Out" behavior is a distinctive signature of the most distant objects and has been used in initial identification of all the most distant quasars, galaxies and GRB.

The center of the image recorded contains an extraordinary gamma-ray burst (GRB) called GRB 110328A, observed with NASA's Chandra X-ray Observatory. This Chandra observation confirms the association of GRB 110328A with the core of a distant galaxy and shows that it was an exceptionally long lived and luminous event compared to other GRBs.

The position of a faint galaxy - located about 3.8 billion light years from Earth - observed with NASA's Hubble Space Telescope and the Gemini-North telescope on the ground. Allowing for experimental errors, the position of the galaxy is indistinguishable from that of the X-ray source, showing that the source is located close to the middle of the galaxy. This is consistent with the idea, suggested by some astronomers, that a star was torn apart by a supermassive black hole at the center of the galaxy. This idea differs from the usual interpretation for a GRB, involving the production of a jet when a black hole or neutron star forms after the collapse of a massive star ($30M_{\odot}$ or more) or a merger between two neutron stars.

<http://chandra.harvard.edu/resources/illustrations/blackholes2.html>

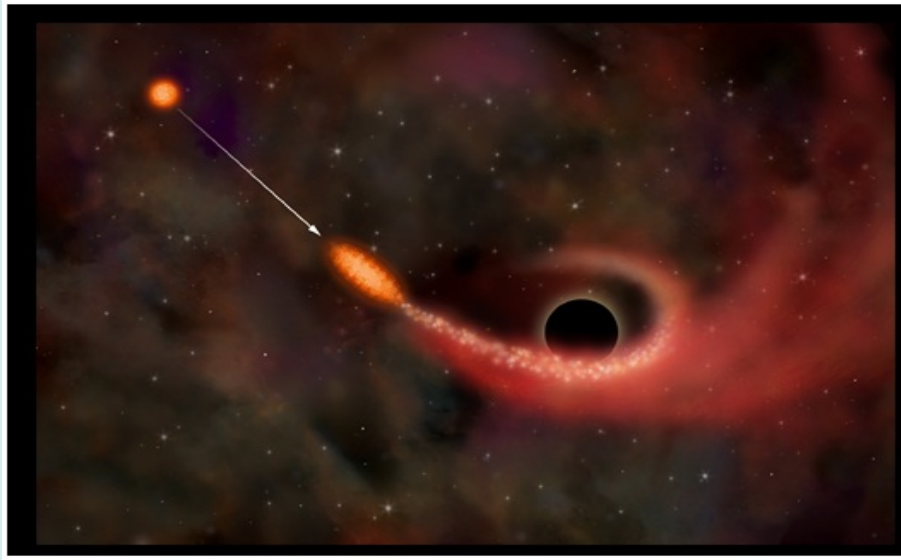


Figure E1: Sun-size star, after being born at aG1 the first geo-synchronous orbit, is launched on a collapsing spiral orbit around the nucleus of the Super Massive Black Hole. (Illustration: NASA/CXC/M.Weiss).

The first illustration in this sequence shows a doomed star (orange circle) that is launched on a death spiral around SMBH. The black hole's enormous gravity stretches the star until it is torn apart. Some of the disrupted star's mass (indicated by the white stream) is swallowed by the black hole, while the rest is flung away into the surrounding galaxy.

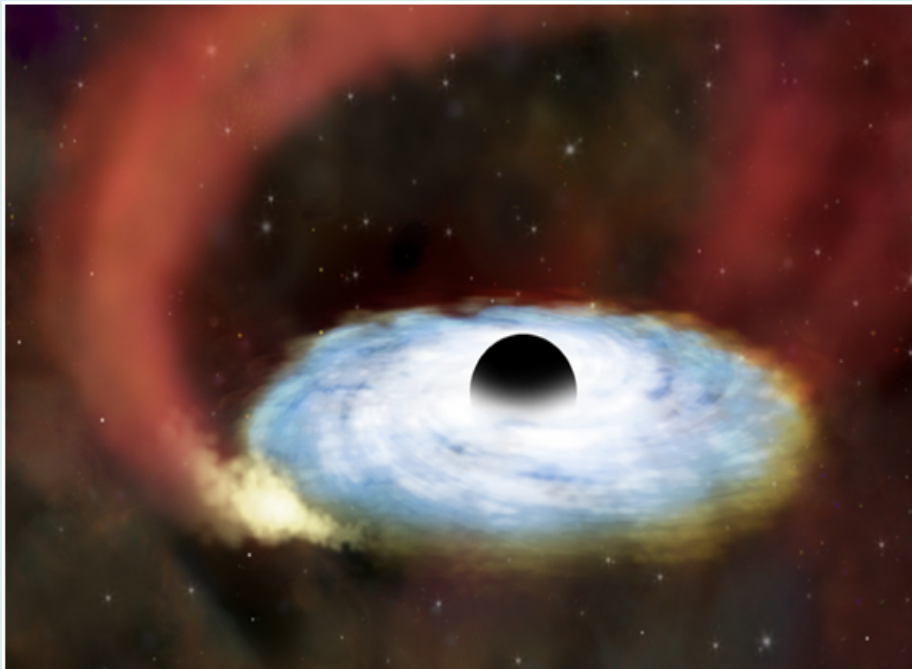


Figure E2: Fraction of the star's mass which is gobbled up by the SMBH is spread into a disk called accretion disk around the SMBH. The inner edge of the accretion disk is defined by Innermost Stable Circular Orbit (ISCO) which is defined by Kerr Metric Analysis. Kerr Metric Analysis takes into account the curvature in Space Time Fabric and the Frame Dragging effect in near vicinity of a Super Massive Black Hole. In fact Risaliti, have accurately pinned down the spin parameter of the SMBH in NGC1365 by carefully analyzing and measuring the inner edge of the Accretion Disk (Illustration: NASA/CXC/M.Weiss).

The second illustration shows how the gas that was pulled towards the black hole forms a disk and is heated before being swallowed by the black hole.

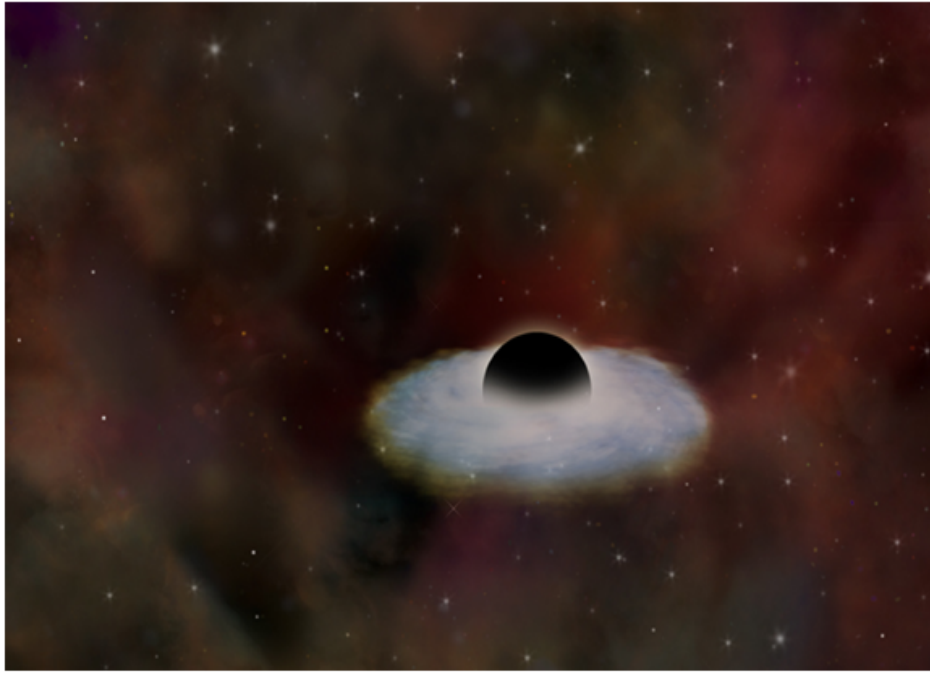


Figure E3: The much fainter disk after about ten years have passed when most of the gases has been swallowed up. (Illustration: NASA/CXC/M.Weiss).

The third illustration shows a much fainter disk, after about ten years have elapsed, when most of the gas has been swallowed by the black hole.



Figure E4: A normal star in the given Galaxy after being born at 'aG1' is launched on a death spiral around the black hole. (Illustration: NASA/CXC/M.Weiss).

A star, marked yellow, is born at 'aG1' and by perturbative forces is launched on death spiral around a giant black hole in the center of the galaxy RX J1242-11.



Figure E5: The doomed star spirals inward on a collapsing spiral orbit around the SMBH. (Illustration: NASA/CXC/M.Weiss).

As the doomed star nears the SMBH, the star is stretched by tidal forces exerted by the black hole and is quickly torn apart.

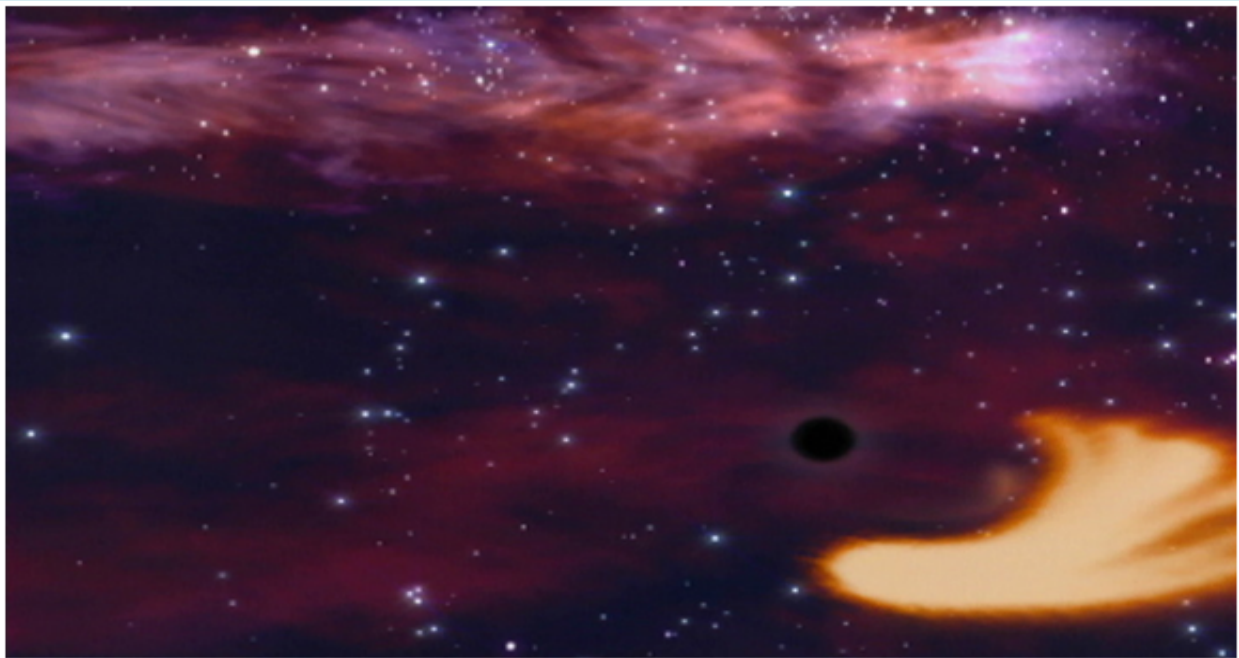


Figure E6: Most of the yellow gaseous debris of the shredded star escapes on parabolic orbits as can be seen in the spread of the yellow debris spiraling in anticlockwise direction. A part of the yellow debris escapes away the BH (Illustration: NASA/CXC/M.Weiss).

Most of the yellow gaseous debris from the star escapes the black hole in parabolic orbits.



Figure E7: A small fraction of the shredded star swirls into the vortex created by the rapidly spinning SMBH. As the remnants of the shredded star is sucked in a swirling motion it gets heated up and emits X-Ray. (Illustration: NASA/CXC/M.Weiss).

However, a small amount of material is captured by the black hole and then forms a rotating disk of gas. X-rays are emitted as the gas in the disk is heated (as shown by the blue color) and is gradually swallowed by the black hole, eventually emptying the disk.

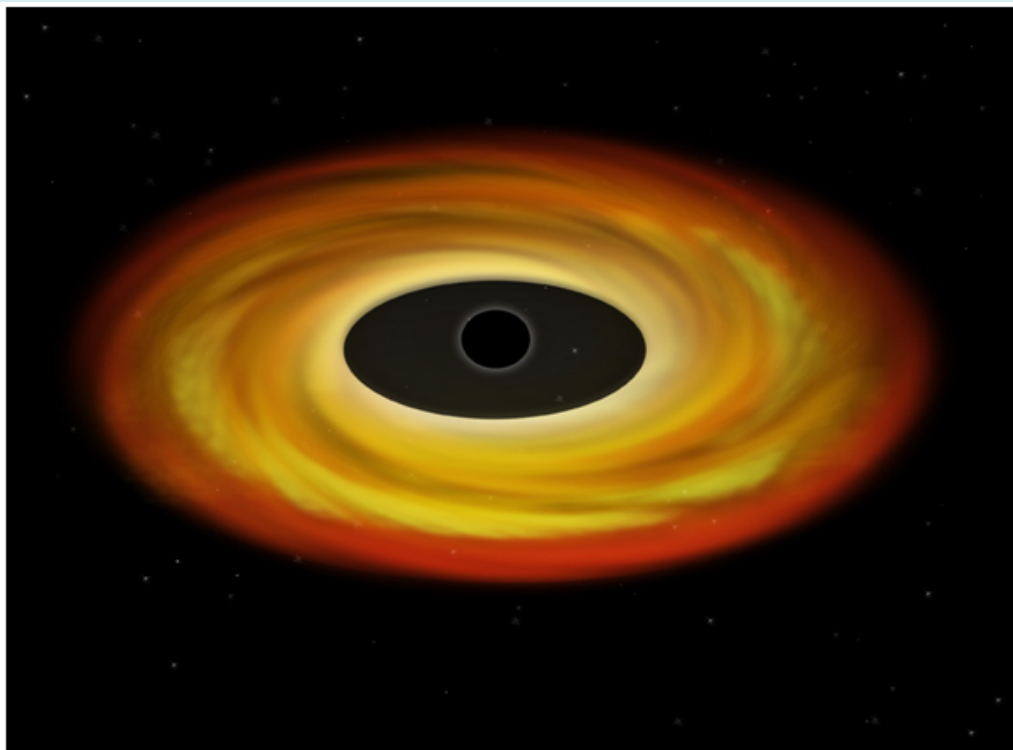


Figure E8: A non-spinning SMBH a consequence of zero inward spiral. (Illustration: NASA/CXC/M.Weiss)

When there is little or no inward spiraling debris, SMBH has little or no spin.

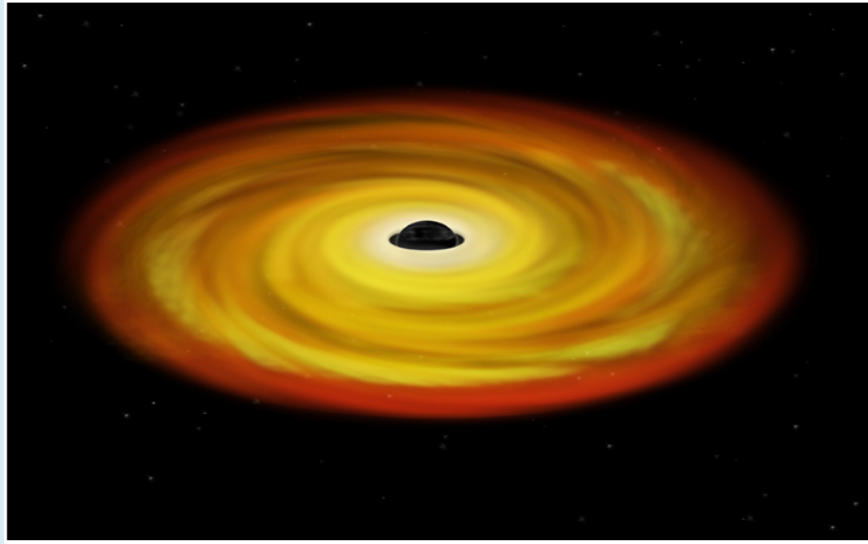


Figure E9: A rapidly spinning SMBH because of enormous inward spiraling debris. Infact an archival record of the spin of the SMBH unfolds the evolutionary history of the SMBH and its host Galaxy. A high spin parameter indicates a history of coherent mergers whereas a low spin parameter indicates a history of chaotic mergers. (Illustration: NASA/CXC/M.Weiss).

As shown in Figure 8 and Figure 9, the gravity of a black hole shifts X-rays from iron atoms to lower energies, producing a strongly skewed X-ray signal. Figure 8 has black hole that is depicted as not spinning, and a second black hole in Figure 9 is depicted as spinning rapidly. One consequence of Einstein's theory of relativity is that spinning black holes drag space with them as they spin, making it possible for particles to orbit nearer to the black hole. A possible explanation for the differences in spin among stellar black holes is that they are born spinning at different rates. Another is that the gas flowing into the black hole spins it up.

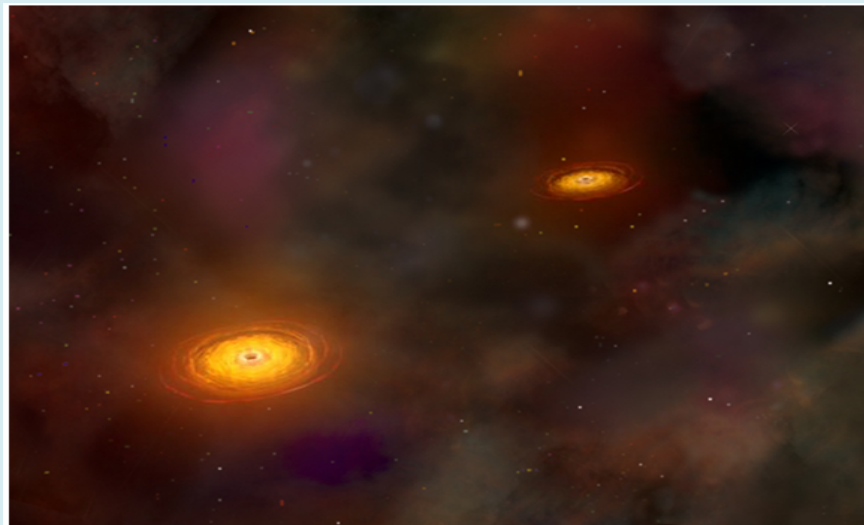


Figure E10: First stage in the merger of two Spiral Galaxies. (Illustration: NASA/CXC/M.Weiss).

The first stage in the merger of two spiral galaxies. In a cluster, galaxies are hierarchically arranged just as in a galaxy stars are hierarchically arranged. The heaviest galaxy with the largest SMBH form the nucleus or the primary body of the cluster and the lighter galaxy forms the secondary body in the cluster. The secondary Galaxy, if it falls short of the inner geo-synchronous orbit, is bound to be launched on a collapsing spiral orbit and thereby get trapped in a death spiral. These two Galaxies are destined for merger.

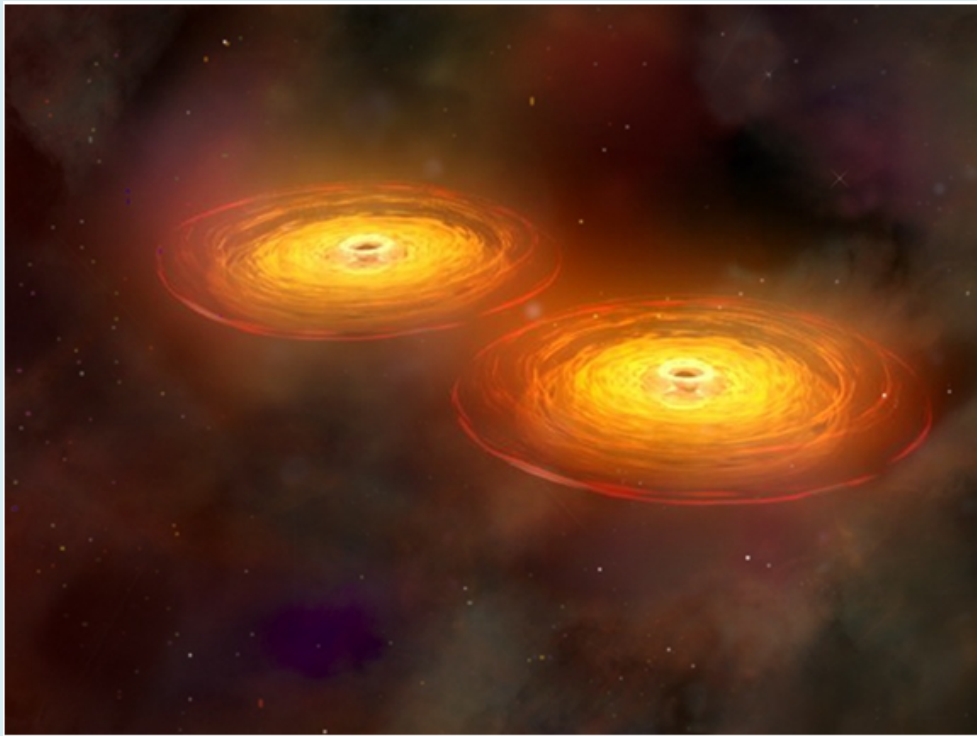


Figure E11: Second stage in the merger of the primary and secondary Galaxies. The two galaxies are spiraling around the barycenter and moving closer together. (Illustration: NASA/CXC/M.Weiss)

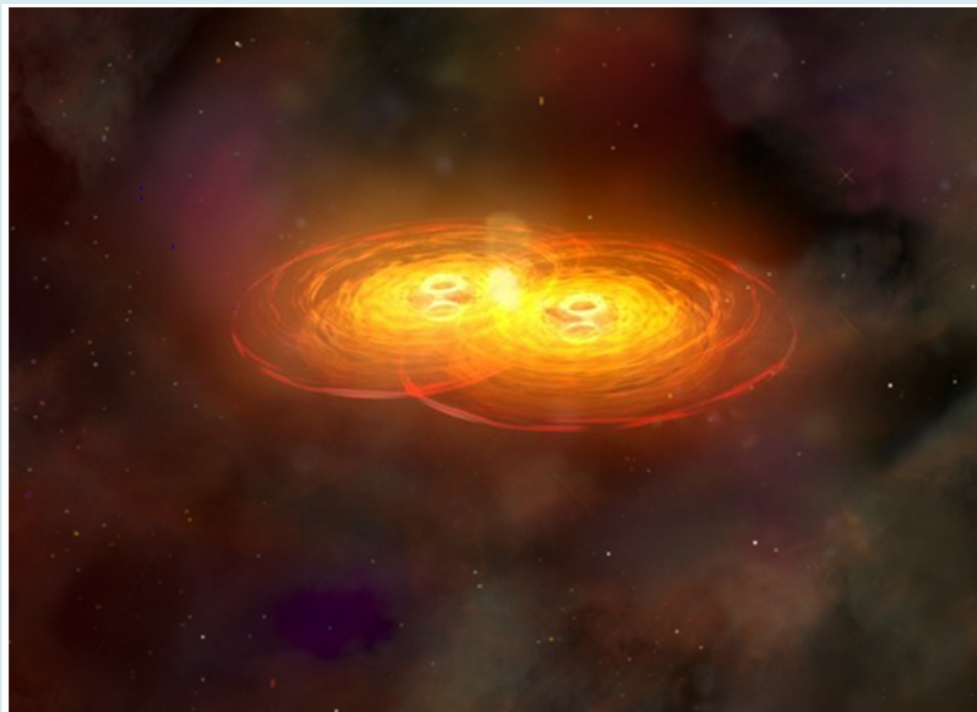


Figure E12: In the advanced stage of merger when the two Galaxies are overlapping and interpenetrating. The two SMBHs are distinguishable surrounded by a single merged Galaxy. (Illustration: NASA/CXC/M.Weiss)

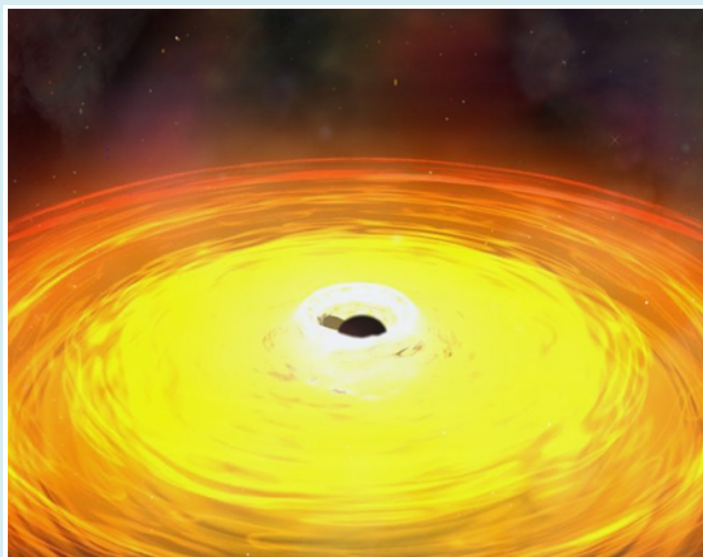


Figure E13: The two SMBHs spiral around the common barycenter until they coalesce into a single SMBH. The final merger of the two SMBH gives rise to the short duration Gamma Ray Burst which so often are recorded by terrestrial Scientists (Illustration: NASA/CXC/M.Weiss).

This series of Figures (Figures 10-13) depict 4 stages in a merger of two galaxies (artistic representation) that forms a single galaxy in Figure E.13 with two centrally located supermassive black holes surrounded by disks of hot gas. The two black holes orbit each other for hundreds of millions of years in Figure E12 before they merge to form a single supermassive black hole in Figure E13 that sends out intense gravitational waves.

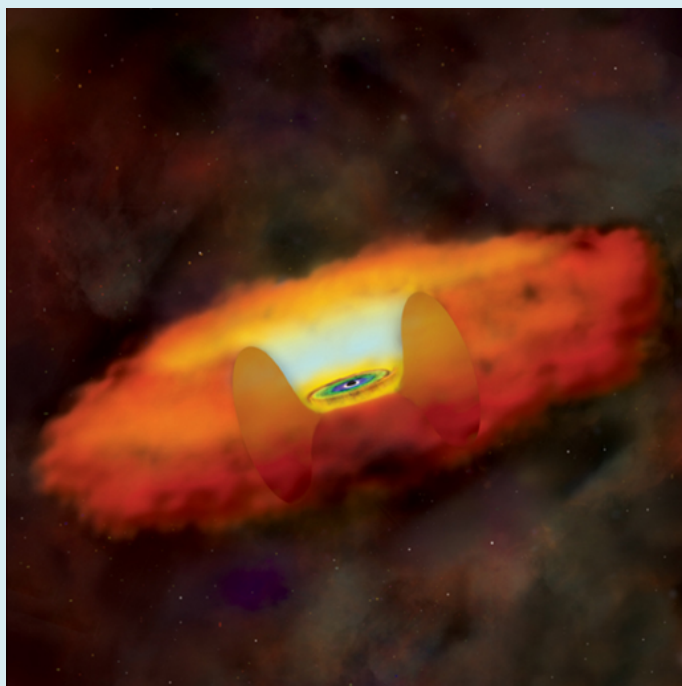


Figure E14: An active galactic nucleus (AGN). AGN refers to QUASERS. Galaxies with turned on SMBH at the center give out an enormous amount of energy in RF range. These are referred to as Quasi-Stellar Radio Sources. In fact QUASERS are radiative manifestation of SMBH (Illustration: NASA/CXC/M.Weiss).

When we look down along the relativistic jet then AGN is referred to as Blazars. When we see at 30 degree angle with respect to the jet we call it QUASER. When we see it at 60degree angle we refer to AGN as Seyfert1 and when we see it at 90 degree we call it Seyfert 2 or Radio Galaxy.

An artist's conception shows a black hole surrounded by a disk of hot gas, and a large doughnut or torus of cooler gas and dust. The light blue ring on the back of the torus is due to the fluorescence of iron atoms excited by X-rays from the hot gas disk.

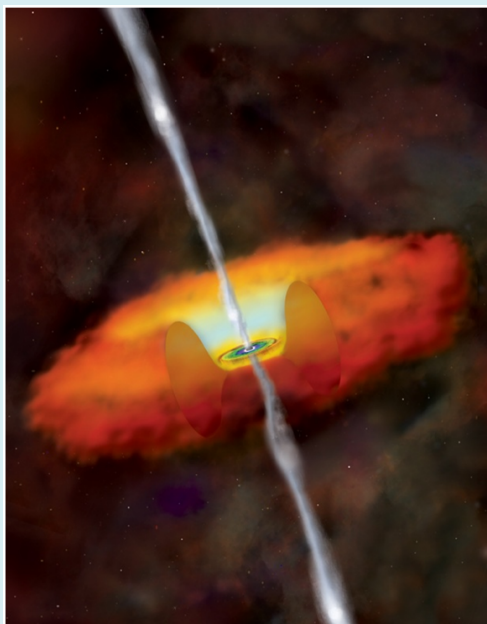


Figure E15: An emission of conical beam of energetic charged particles and X-Rays from the north and south pole of AGN due to swirling mass of gas and dust into the rapidly spinning SMBH. This is the turned on stage of SMBH. When little or no accretion there is no relativistic jet and we say that SMBH is in quiescent stage.(Illustration: NASA/CXC/M.Weiss).

An artist's conception shows a black hole surrounded by a disk of hot gas, and a large doughnut or torus of cooler gas and dust. The light blue ring on the back of the torus is due to the fluorescence of iron atoms excited by X-rays from the hot gas disk. Jets of high energy particles (white) are propelled away from the vicinity of the black hole by intense electric and magnetic fields.

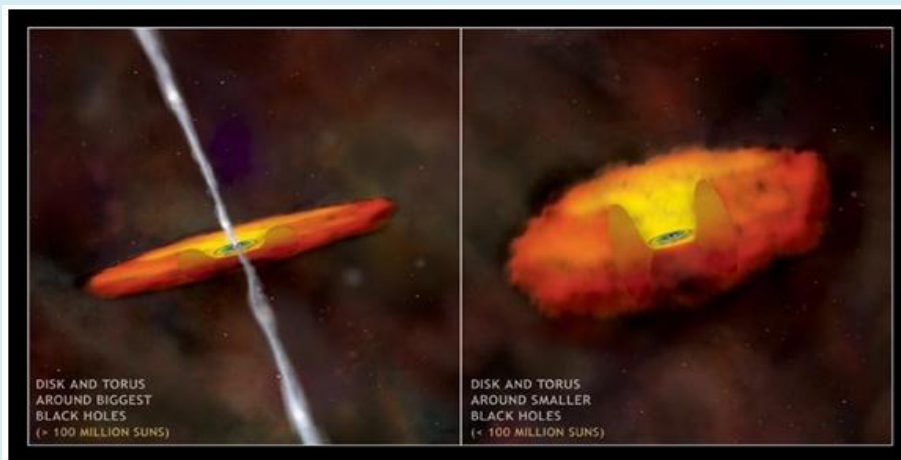


Figure E16: Left SMBH is greater than 100 Million Suns. It has thinner torous and a powerful beam of energetic particles emanated from the two poles of the SMBH. Right SMBH is between 10 Million Suns and 100Million Suns. It has a much thicker donought of gas and dust and no conical emission from the two poles (Illustration: NASA/CXC/M.Weiss).

Figure E16 shows two kinds of AGNs. These two show the difference between the very biggest supermassive black holes in the Universe and relatively smaller ones. In each case, the black hole is swallowing large amounts of gas from a surrounding disk. The first illustration (Right Hand Side) is of a black hole with a mass between about 10 million and 100 million Suns. Here, the central black hole is obscured by a thick donut-shaped cloud of dust and gas. The second (Left Hand Side) shows the growth of a larger black hole, with a mass greater than 100 million Suns. This black hole is surrounded by much a thinner torus of dust and gas and has a powerful beam of conical beam emanated from the two poles of SMBH.



Figure E17: Black-hole size versus Cosmic time in very early Universe (Illustration: NASA/CXC/M.Weiss).

In early universe Super Massive Black Holes and Super Massive Galaxies grew synergic ally. Subsequently Massive Black Holes and Massive Galaxies were formed. Figure F.17 shows the typical growth, over cosmic time, of supermassive black holes with masses greater than 100 million Suns (these objects include the largest black holes in the Universe). These large black holes grow quickly in the early Universe but their growth then stops (“hits the wall”), perhaps because powerful winds or jets generated by the feeding frenzy of the black holes clears out any remaining fuel. The rapid, early growth of these large black holes, as observed with Chandra, is similar to the growth of their large host galaxies, as observed with optical telescopes.

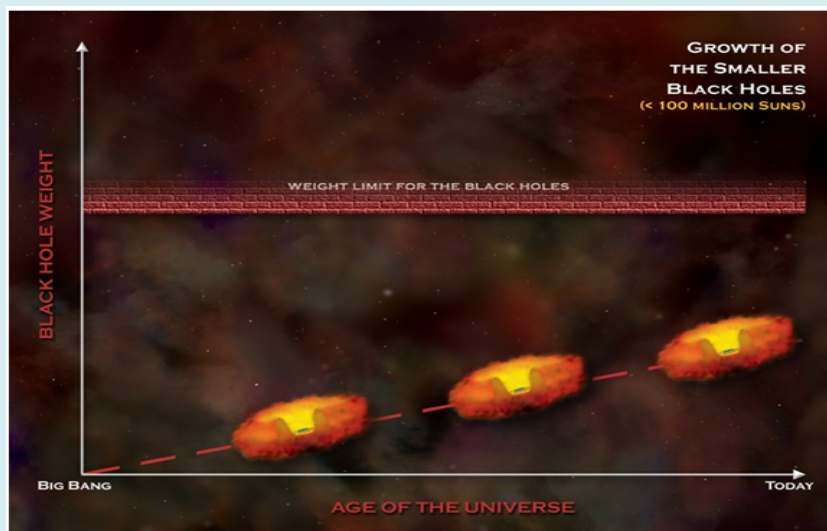


Figure E18: Black hole size versus Cosmic time in later times. (Illustration: NASA/CXC/M.Weiss).

Figure E18 shows the typical growth of super massive black holes with masses less than about 100 million Suns. These black holes grow much more slowly than the biggest black holes. Typically they will not reach their weight limit for another several billion years. This slow growth is similar to the growth of the black holes' host galaxies.

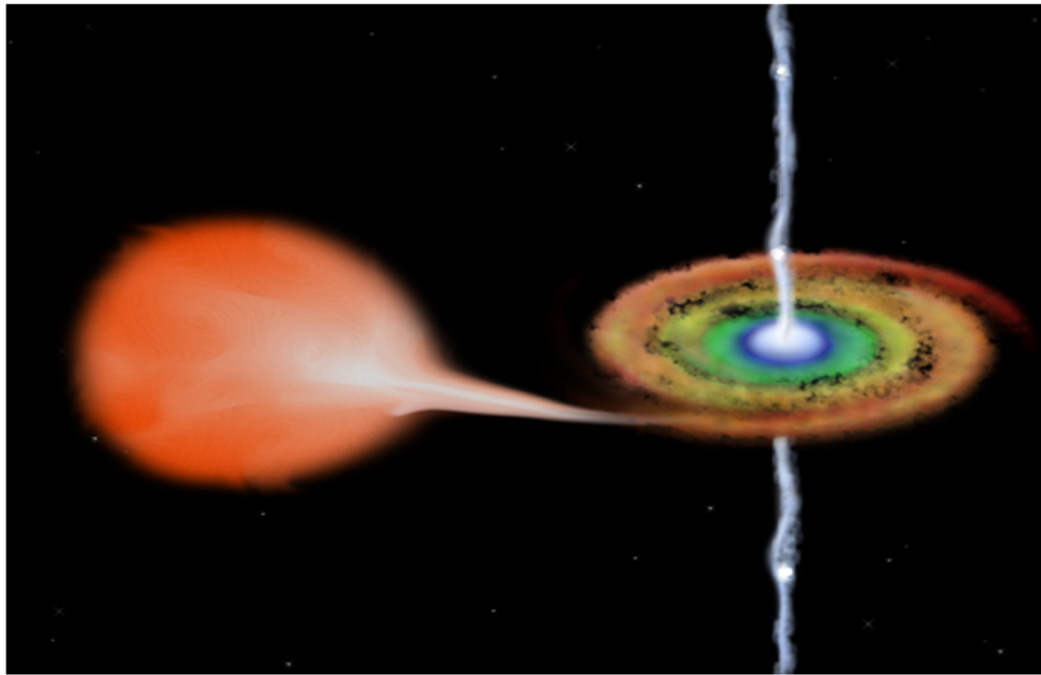


Figure E19: A double star system of Sun-like star and BH (Illustration: NASA/CXC/M.Weiss).

In a double-star system of normal star and BH, normal star is a secondary body and BH is primary body. If the secondary is launched on an expanding spiral orbit it rapidly evolves to a stable orbit at aG2. But if it is launched on a contracting spiral the star gets trapped on a death spiral doomed to be shredded and devoured by the SMBH and in the process emanate a powerful polar cone of energetic particles, X-rays and γ -rays. This is tidally disrupted event accompanied by big, intense and long duration gamma and X-ray burst. In double star system where a normal Sun-like star is in orbit around a black hole, as gaseous matter is pulled from the normal star it spirals toward the black hole, forming a disk, and is heated to temperatures of millions of degrees. Intense electromagnetic forces in the disk can expel jets of high-energy matter.

GRB110328A was of the category shown in Figure F.19. Joshua Bloom sent a email GCN 11847 on GRB Coordinates Network (GCN). He suggested that it was not a typical GRB associated with the collapse of a massive star into a neutron star or into a black hole neither it was a GRB associated with the merger of two neutron stars. It was an event associated with a tidally disrupted event (TDE) of a sun-sized star by a million sun mass SMBH. GRB was coincident with the nucleus of the Galaxy. This was rechristened as SW1644+57. The Chandra data pinpoints GRB110328A in the core of this galaxy and shows that the associated X-ray source is very bright and long-lived.

A normal GRB can occur anywhere in the galaxy where star formation is active.

Most MBH or SMBH are quiescent or dormant without the swirling mass of gas and dust surrounding it.

MBH can have a disc of gas and dust swirling into the rapidly spinning vortex created by MBH. This wirling mass gets heated up and emits high energy particles, X-Rays and some emit γ -Rays also. These are known as Active Galactic Nuclei (AGN) as shown in Figure F.14 and Figure F.15. These are active because they are continuously fed by gaseous and dust matter. These AGN are also called QUASERS. In about 10% of galaxies we have AGN.

AGN are easy to detect because of their X-Ray emission and some have weak γ -Ray emission also. But SW1644+57 is a class apart. It is 100× brighter than AGN.

Before 28 March 2011, Sw1644+57 was quiescent as confirmed from the data of Fermi Satellites Large Area Telescope (LAT). Only when a star spiraled into 'the disruptive radius' sphere of an otherwise quiescent SMBH that long duration GRB was triggered from the relatively slow tidal disruption of the doomed star. 10% of the debris from the shredded star was converted into X-Ray and γ -Ray (typical accretion efficiency of the BH = $\epsilon_{\text{BH}} = 10\%$).

During TDE UV, X-ray, Visible light have been seen but γ -Ray had never been seen.

Sw1644+57 has unique brightness and variability of X-Rays after-glow. It flared 5 times since April 3, 2011. The burst of X-Ray and γ -Ray is stronger than 1000 to 10000 times. This flare up will not happen again because star had been fully swallowed.

Mass of BH			
$>10^8 M_{\odot}$	Disruption Radius < Event horizon	TDE will be hidden	No relativistic cone
$<10^8 M_{\odot}$	Disruption Radius > Event horizon	TDE will be seen	Relativistic cone is detectable
$\sim 10^8 M_{\odot}$	Disruption Radius > Event horizon	TDE will be seen	Relativistic cone is detectable

Table E1: Comparison of TDE occurring in SMBH and MBH.

Sw1644+57 shows that there is a new class of TDE. Though it was detected because of Gamma burst, its behavior at X-Ray and IR was unique. It stayed at a high flux level for days to weeks. This puts it in a class apart from known high energy transients.

Remarkably, this "tidal disruption" event may have been caught in real time, rather than detected later from analyzing archival observations. However, this X-ray source is about a hundred times brighter than previously observed tidal disruptions. One possible explanation for this very bright radiation is that debris from the disrupted star fell towards the black hole in a disk and the swirling, magnetized matter generated intense electromagnetic fields that created a powerful jet of particles. If this jet is pointed toward Earth it would boost the observed brightness of the source. This scenario has already been suggested by observers to explain the bright and variable X-ray emission observed by NASA's Swift telescope.

This observation was part of a so-called target of opportunity, or TOO, led by Andrew Levan from the University of Warwick in the UK. A TOO allows the telescope to react quickly to unpredictable cosmic events, within 24 hours in some situations. Chandra scientists and engineers can decide to alter the scheduled observations and instead point the telescope to another target if the circumstances warrant it. This process was put into place once the discovery of GRB 110328A with Swift was announced on March 28th, 2011. The Chandra team was able to reset the telescope's schedule to observe GRB 110328A early in the morning of Monday, April 4th for a period of just over four hours.

Results of Levan Group

An extremely luminous panchromatic outburst, a high-energy transient, was seen on the night of 28 March 2011. This will be referred to as Sw1644+57. There are several candidates which can produce sufficiently bright bursts of high radiation such as:

- Electrical discharges associated with thunderstorms on Earth;
- Some fraction originate from the Milky Way : (a) from isolated neutron stars with intense magnetic field or (b) from binary systems containing neutron stars and black holes;
- Some long lived but variable X-Ray and γ -ray emissions originate in active galaxies;
- Brightest are the long duration γ -ray bursts (long-GRB) which are detected by SWIFT-mission at a rate of approximately two a week and thought to originate from the collapse of massive stars in the distant Universe.

Even among the long-GRB observed till now, the present candidate Sw1644+57 manifests some unusual properties as shown

in Table E2 r_s (Schwarzschild radius) = $\frac{2GM_{\text{BH}}}{c^2}$

	Long-GRB	Sw1644+57
	Destructive event and non-repetitive	
Prompt γ	1~10 sec	
Emission duration.		
Subsequent trigger	zero	4 triggers over a period of 48 hours
Late time X-Ray flare	Yes	Quite unlike the afterglow of long-GRB (0.3 to 10keV)

Peak X-Ray flare		3×10^{48} ergs/s Persisted for 1000s.
Light curve of X-Rays emission in 0.3 to 10 keV	Plateau phase of 9 hours	Plateau Phase maintained till 5 weeks
IR light curve	Very faint in afterglow	Plateau Phase for 5 weeks
Luminosity in after-glow for X-Ray and IR	X-Ray luminosity is much less and IR is faint	Persisted at $L_x \sim 10^{47}$ erg/s and persisted for 2 weeks. 10-100 times more luminous in X-Ray & IR.*
Total energy emitted in first 10^6 sec	Much less than 10^{53} ergs	10^{53} ergs = 10% of the rest energy of SUN
Afterglow Astrometric position	Highly correlated with host galaxy light (particularly with the blue light generated by massive stars)	Coincident with the nucleus of the galaxy

Table E2: The comparative study of Long-GRB and Sw1644+57.

*Sw1644+57 is well beyond the bright end of the quasar luminosity function and 100 times more luminous than the brightest Blazer.

The overall energetic, long duration, together with order-of-magnitude variation in flux over 100s time scale indicate that we are dealing with a very different class of high energy transient.

These differences show that Sw1644+57 is not a classical long-GRB. Then where does it fit?

Below in Table E3, we describe different classes of AGNs

Class of AGN	Properties
LINERS & Seyferts	Moderate X-Ray and optical luminosity
Luminous QUASARS & blazars	Brighter AGN
Blazars	X-Ray Luminosity approaches 10^{46} ergs/s and
	Optical absolute magnitude is -30 or brighter.
	Light curve has a variability of a factor of 2 hence this is considered as most variable AGN.
Sw1644+57	Peak X-Ray luminosity is in excess of 10^{48} ergs/s.
	In just a few hundred seconds it has a light curve variability of 100.
	Extremely X-Ray luminous but optical & IR Luminosity is much fainter.
	Spectrally unusual.
	X-Ray /Optical Luminosity $\sim 10^4 \sim 8$;

Table E3: Classification of AGNs.

The host galaxy is compact and non-interacting with (half-light radius in the optical range) $r_h = 1.04$ kpc and absolute magnitude of $M_V = -18.9$. This is comparable to Large Magellanic Cloud (LMC) Galaxy. The study of emission lines show that it is normal star forming Galaxy which had a dormant SMBH at the nucleus. The inferred rate of formation of stars is $0.5 M_\odot$ per year.

Peak Luminosity corresponds to Eddington Luminosity of the accretion by $10^{10} M_\odot$ mass Black Hole. But Stellar Mass-Black Hole Mass relation indicates that central Black Hole is $10^7 M_\odot$. Hence Sw1644+57 is either accreting at a super-Eddington rate or has its total energy modified by a relativistic beaming or both.

Results of Bloom Group

If a star happens to enter the sphere of influence of a centrally located BH in a given galaxy then the star will be tidally shredded and almost half of the shredded star will be accreted by the BH at a typical accretion efficiency of 10% and remaining half will be deflected away tangentially. The disruption radius of the BH is given by Equation E.1.

$$r_d (\text{disruption radius}) = R_o \times \left(\frac{M_{BH}}{M_o} \right)^{1/3} \quad (E1)$$

Where R_o = radius of a Sun-like star = $6.955 \times 10^8 \text{m}$; M_o = mass of a Sun-like star = $1.9891 \times 10^{30} \text{Kg}$; M_{BH} = mass of the central black-hole = $10^M \times M_o$;

A centrally located BH has an event horizon. The radius of this event horizon is given by Schwarzschild Radius. The escape velocity ($v_{esc} = \sqrt{(2GM)/R}$) from the sphere surrounded by this event horizon is the speed of light 'c' hence even light cannot escape from within this event horizon, Schwarzschild Radius is given by the expression in Equation E2.

$$r_s (\text{Schwarzschild radius}) = \left(\frac{2GM_{BH}}{c^2} \right) \quad (E2)$$

Where $G = 6.673 \times 10^{-11} \text{m}^3 \text{Kg}^{-1} \text{sec}^{-2}$; c = velocity of light; M_{BH} = mass of the central black-hole = $10^M \times M_o$;

In Table E4, the comparative values of the disruption radius and event horizon radius are given for the various values of the central BH.

Mass of BH ($\times M_o$)	Disruption Radius(m)	Schwarzschild Radius(m)
10^5	3.2×10^{10}	2.95×10^8
10^6	6.92×10^{10}	2.95×10^9
10^7	1.49×10^{11}	2.95×10^{10}
10^8	3.2×10^{11}	2.95×10^{11}
10^9	6.9×10^{11}	2.95×10^{12}
10^{10}	1.49×10^{12}	2.95×10^{13}
10^{11}	3.2×10^{12}	2.95×10^{14}
10^{12}	6.9×10^{12}	2.95×10^{15}

Table E4: Comparative values of Disruption Radius and Schwarzschild Radius for different masses of centrally located BHs.

As can be seen from the Table E.4 for BHs lighter or equal to $10^7 \times M_o$, the Event Horizon Radius is much less than the Disruption Radius hence Tidally Disrupted Flare can be recorded, and Tidally Disrupted Event is observable. If there was a heavier BH, then possibly the event could not have triggered the Burst Alarm Telescope, and the event would have gone unnoticed and unrecorded. Fortunately, this was not the case for GRB110328A.

X-Ray after-glow persisted for more than 2 weeks and its peak luminosity was $3 \times 10^{47} \text{ergs/sec}$. These two features put this event in a class of scaled down version of Blazars which was impulsively fed by a stellar mass of $\sim 1 M_o$. This event seemed coincident with the nucleus of the host galaxy. This coincidence was confirmed by the following three facts:

- Astrometric coincidence of the associated X-Ray, Optical, IR and Radio transient with the light centroid of the putative host galaxy is strongly indicative of a positional connection to MBH;
- Observed X-Ray variability time scale are consistent with those of an accreting MBH;
- Observed X-Ray flux and spectral hardness is like that observed in Blazars.

By applying Bulge Mass-BH mass and Bulge Luminosity-BH Mass correlations we arrive at $M_{BH} \leq 10^7 M_o$. This is securely under the limit ($\text{few} \times 10^8 M_o$) required for tidal disruption of a solar mass to occur outside the event horizon so that the TDE can be recorded and analysed from outside.

Beaming factor taken into account, the X-Ray luminosity $L_X = 10^{47} \text{ergs/sec}$ is consistent with Eddington Luminosity (where inward gravitational force is balanced by outward radiation pressure) of $10^7 M_o$ MBH.

Archival searches spanning two decades have yielded no evidence for prior AGN activities from Radio to γ -Ray waveband. This confirms that BH turned-on specifically on 28/03/2011 due to near-Eddington accretion rates at the time of Burst Alert given by BAT of Swift Satellite. This turning-on launched a relativistic outflow of energetic particles and photon.

This sudden increase in accretion cannot result from gas entering the sphere of influence (soi) because the time scale of

$$\sim \frac{R_{\text{soi}}}{\sigma} \geq 10^4 \text{ years}$$

Where $\sigma = 100 \text{ km/sec}$ (typical bulge velocity dispersion); $\text{MBH} = 10^7 M_\odot$;

$$G = 6.673 \times 10^{-11} \text{ m}^3 \text{ Kg}^{-1} \text{ sec}^{-2}$$

Hence this event can only be Tidally Disrupted Flare (TDF).

The observed energy output is compatible with the mass accreted over a time period of 50 days. This can be verified by the following analysis:

The observed X-Ray fluence SX suggests an energy release of $E_X = 1.6 \times 10^{53} f_b$ ergs over a period of 50 days.

Beam forming factor $= f_b = 5 \times 10^{-3}$ hence the available energy $E_{\text{av}} = 8 \times 10^{50}$ ergs.

This energy is coming from the accretion of the tidally shredded star. We have seen that in such TDE only 50% of the matter is accreted. Hence only $0.5 M_\odot$ will be converted into energy through matter-energy conversion equation with 10% accretion efficiency (ϵ_{BH}). Hence the energy got is:

$$\frac{1}{2} M_\odot c^2 \times \epsilon_{\text{BH}} = 8.95 \times 10^{46} \text{ J} \times 0.1 = 8.95 \times 10^{52} \text{ ergs} \sim 10^{53} \text{ ergs}$$

If we take into consideration that mass gets lost through circularization as well due to disk wind the matter to energy conversion easily accounts for the observed energy of 10^{51} ergs.

This Eddington rate accretion accompanied with matter to energy conversion powers a two-sided jet of relativistic energetic particles and photons. This plows through the interstellar region surrounding BH at a Lorentz Factor Γ_j . At some later time jet reaches a distance R_j where the forward shock radiates the observed radio and IR light.

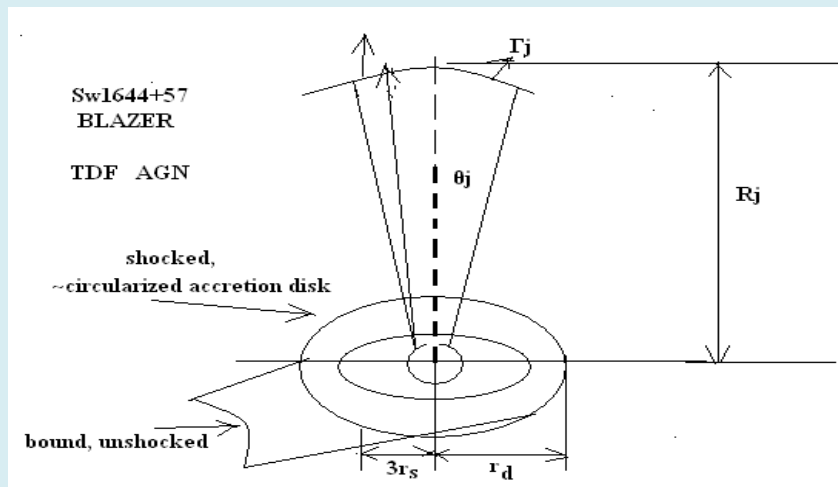


Figure E20: Schematic representation of the geometry and emission region for Sw1644+57. A star is disrupted at a distance of r_d from a MBH of mass MBH with Schwarzschild Radius r_s . Half of the mass of the star escapes on unbound orbits while the other half accretes. Shocked circularized fall back mass sets up a temporary accretion disk with inner radius of $3r_s$. (for a non-spinning BH). A two sided jet is powered starting at the time of accretion and plows through the interstellar region surrounding the BH at a Lorentz factor Γ_j . At some later time the jet has reached a distance R_j where forward shock radiates the observed radio and IR light. Emission from the accretion disk is upscattered, giving rise to the observed X-Rays. Different viewing angles (whether the observer is inside $\theta_j = 1/\Gamma_j$) determines the class of Blazer we observe.

Emission from the accretion disk is Compton Scattered giving rise to the observed X-Rays. Differing viewing angles (whether the observer is inside $\theta_j \approx 1/\Gamma_j$ or not) determine the sort of phenomena we observe.

The duration of X-Ray light curve and the requisite accretion rate also are broadly compatible with the several days fall back time.

Overall Spectral Energy Distribution (SED) displays two peaks: one for IR and the other for X-Ray/ γ -Ray. This is reminiscent of the Blazars. Low energy is modeled as Synchrotron Emission and high energy is modelled as Inverse Compton (IC) emission.

X-Ray emission shows bright/flaring and a dim/slower flaring (quiescent state). Under TDF hypothesis, the observed SED is explained as follows:

- Synchrotron origin for Radio Emission;

$$\frac{\nu F_{\nu} \text{ luminosity of low energy peak}}{\nu F_{\nu} \text{ luminosity of high energy peak}} = \frac{1}{10} \sim \frac{1}{100}$$

- As in Blazars, here IR is synchrotron emission and X-Ray Peaks are IC emission. The extreme ratio and relatively low frequency of the synchrotron peak are compatible with Eddington-accreting Blazer emission;
- Rapid variability of X-Ray emission strongly indicates of internal origin. The Radio-IR emission varies more smoothly and could result from the interaction of the Jet with the surrounding interstellar medium. Since there was no previous AGN activity hence the jet must burrow its way through the gas in the central region of the Galaxy. The fast motion of the newly formed jet drives a shock into the external gas (forward shock) while simultaneously a reverse shock slows it down. Particles acceleration at these shocks may power afterglow emission simultaneously with jet formation and yet persist beyond the fading of internal emission.

This model, shown in Figure E20, best accommodates the data and predicts the long term evolution of Radio and IR transient. If TDF hypothesis is correct, emission will fade over the year and will not repeat because all the accreting material would have exhausted by then.

The emerging jet from the tidal disruption event appears to accelerate cosmic rays to the highest observed energy (10^{20} eV). The observed rate of jets associated with tidal disruption of stars is $dR/dt \sim 10^{-11} \text{Mpc}^{-3} \text{year}^{-1}$. Energy released per event is $3 \times EX \sim 5 \times 10^{53} \text{erg}$. Energy injection rate is $dE_{\text{TDF}}/dt \sim 5 \times 10^{42} \text{ergs Mpc}^{-3} \text{year}^{-1}$. The injection rate of energy into the tidally powered cone should be $10^{44} \text{ergs Mpc}^{-3} \text{year}^{-1}$ in order to accelerate the cosmic particles to energy above 10^{19}eV .

There is much evidence that AGN jets are accelerated by Magneto Hydro Dynamics.

Appendix F

Calculation of (Baryonic Matter/Dark Matter)

Launch of COBE (Cosmic Background Explorer) started the era of precision measurement of the Cosmic Microwave Background (CMB) Radiation.

What is CMB?

- According to Big Bang theory, our Universe started from a singularity. It rapidly inflated to a very large size in 10-30 seconds. Its event Horizon expanded faster than light speed. This lasted from 10-43 seconds to 10-35seconds.
- After 10-30seconds. Universe expanded sedately and monotonically [102].
- Initially the four forces (Gravitational forces, Strong forces, Weak forces and Electro-magnetic forces) were of equal magnitude as a single Force as shown in Figure G1.

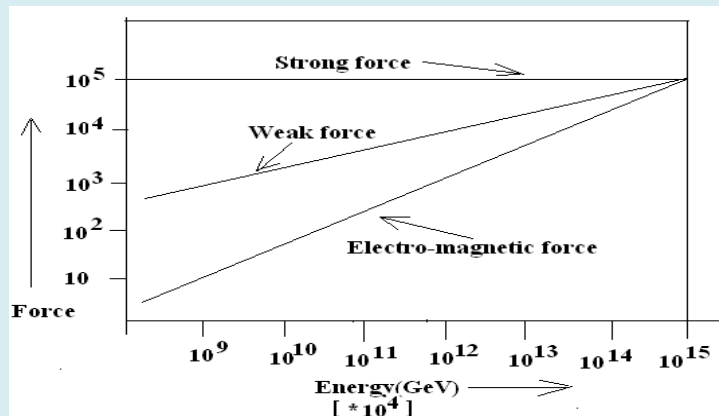


Figure F1: Comparative plot of Strong, Weak and Electro-magnetic forces.

From 0 second to 10^{-43} second, temperature fell from infinity to 10^{19} GeV, radius of the Universe expanded from 0 to 10^{-33} cm. Below 10^{19} GeV, super symmetry is broken, and Universe makes a phase transition from Quantum Gravitation to Grand Unified Phase. Gravitational force decoupled and relic Gravitons were left behind which we should be able to measure but have not been able to measure till now.

From 10^{-43} sec to 10^{-35} sec, the Universe experienced an inflationary expansion. The event horizon surrounding the singularity expanded at a speed greater than the speed of light.

By 10^{-30} sec, Universe expanded from a singularity of zero dimensions to a baseball size sphere. After this, Universe expanded sedately and monotonically. The inflationary phase was over.

At 10^{-10} sec, the temperature fell to 100 GeV. There is phase transition from Grand Unified Phase to Electro-weak phase. Weak force decouples and relic Intermediate Vector Bosons W^+ , W^- and Z^0 are left behind. Below 100 GeV, weak forces and electromagnetic forces are separated. This phase transition is also known as Salam-Weinberg Transition in honour of Abdus Salam and Steven Weinberg who worked out the electro-weak theory.

At 10-6sec, the temperature fell to 1 GeV. Below 1 GeV, there is Quark-Nucleon Phase transition. Strong forces get decoupled, quarks are confined to baryons (which are triplets of quarks) and mesons (which are doublets) and relic quarks are left behind. Baryons are the nuclear particles like protons and neutrons and mesons mediate the strong force within a nucleon. In this decoupling residual quarks are left behind as relic quarks which should be detected with its abundance as high as that of gold but till date no relic quark has been detected.

380,000 years after the Big-Bang the temperature of the hot soup known as plasma, the fourth state of matter, consisting of protons, neutrons and electrons falls to 4000K. Below 4000K, plasma gets neutralized into a neutral gaseous mixture of H_2 and He. Radiation decouples leaving behind relic photons. Today after 13.7 Gy, these Relic Photons have cooled to 2.7K Black Body Radiation. This 2.7K Black Body Radiation is known as Cosmic Microwave Background Radiation (CMB radiation).

For 380,000 years after the Big Bang, matter was in a plasma state and, through Compton Scattering, matter and photon were kept in thermal equilibrium though they had different adiabatic indices. Because of Compton Scattering, photons had the same density distribution as the matter density distribution. When temperature fell below 4000K, matter and radiation got decoupled and matter changed from ionized state to neutral state. Since the two cooled independently, Temperature of matter fell inversely as the square of the Radius of the Universe and temperature of radiation fell inversely as the Radius of the Universe. But the Black body Radiation carried the imprint of the matter density distribution at the time of parting at 380,000 years after the Big Bang.

Subsequently matter has evolved as a very differentiated and non-homogeneous system of super-clusters, clusters, galaxies and as exo-solar systems. If today we have such a non-uniformity of matter distribution then at 380,000 years after the Big Bang we should have the seeds of this non-uniformity and this imprint should be present as ripples in CMB radiation.

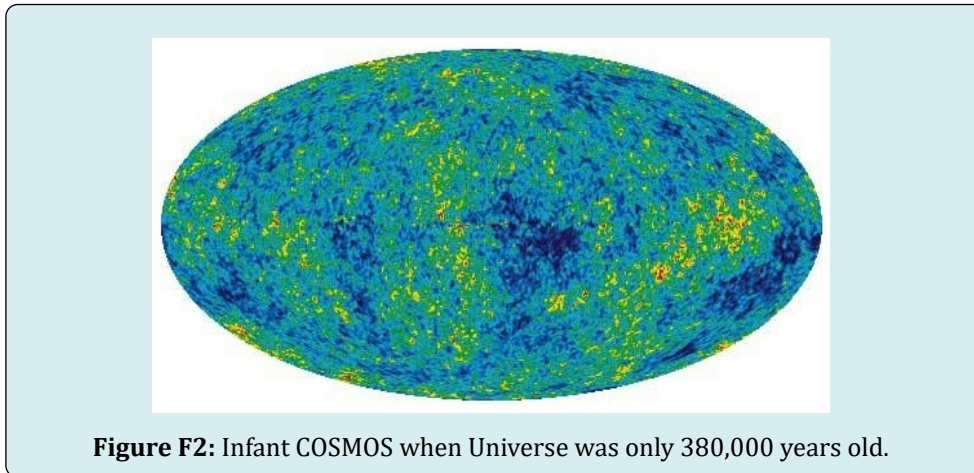
In 1960's AT & T, Bell Lab used a radiometer in a telescope that would track the early communication satellites namely Echo-1 and Telstar. This radiometer was being tested by Arno A. Penzias and Robert W. Wilson. In course of this testing they detected a background noise in microwave spectrum. It corresponded to 2.776K Cosmic Microwave Background Radiation (CMBR). They were led to this idea by the news that Robert H. Dicke had suggested in 1940 that a radiometer would detect this CMBR.

The discovery firmly established the Big Bang Theory. In 1978 the Nobel Prize in Physics was awarded to Arno A Penzias (American), Robert Woodrow Wilson (American) and P.L. Kapiteza (Russian) for the discovery of Cosmic Microwave Background Radiation.

In 1990, a satellite called COBE (Cosmic Background Explorer) measured the spectrum and temperature variations in the radiation pattern. The spectrum was exactly as expected for 2.7K Black Body radiator. The temperature variation was 1 in 100,000. Till then CMB radiation had appeared as perfectly isotropic and isotropic radiation pattern cannot explain the galaxies, clusters and superclusters formation. Therefore the achievement of COBE marked the correctness of the Big Bang Theory.

To refine the CMB radiation pattern studies, in 2001 Wilkinson Microwave Anisotropy Probe was launched (WMAP). This is in a circular orbit around Sun with semi-major axis $a = + 1.5 \times 10^6$ km.

In February 2003, the image of the infant cosmos only 380,000yrs old was received. The results from WMAP reveal that the CMB temperature variations follow a distinctive pattern predicted by cosmological theory: the hot and cold spots fall in characteristic sizes. The image of infant cosmos is shown in Figure F.2.



The hot spots or the red spots in CMB image are the images of compressed, dense plasma region and cold spots or the blue spots in CMB are the signature of rarefied plasma. The red spots will act as the seeds for super clusters. These super-clusters hierarchically gave rise to clusters, clusters gave rise to galaxies and galaxies rise to stars and solar systems.

In July 2003, Scientists superimposed SDSS data on the microwave intensity map developed by WMAP. They conclusively proved that there is what is known as integrated Sachs-Wolfe effect. Clustering of galaxies cause dimple in space- time fabric. Anti- gravity outward push tends to stretch out the dimples in an otherwise flat Universe and in the process tends to crush the Cosmic Microwave Background Radiation at and near the dimples meaning by anti-gravity push shifts the microwave radiation towards shorter wavelength. This precisely was observed in the superimposed map. This is a definitive proof of dark energy dominance in our present Universe.

The results from WMAP have been corroborated by SLOAN Digital Sky Survey(SDSS) and by Supernovae Cosmology Project and they are the following:

- There is 4% ordinary Baryonic matter, 23% dark matter composed of exotic particles and 73% dark energy;
- The Hubble Constant has been nailed at $H_0 = \text{Rate of expansion of our Universe} = 71 \text{ Km}/(\text{sec-Mpc})$;
- The age of our Universe is fixed at 13.7Gy;
- Supernovae Cosmology Project is consistent with Flat Universe with Cosmology Constant being non-zero and positive.
- The result that there is 4% Baryonic Matter and 23% Dark Matter tells us that:
- ordinary matter: dark matter = 1: 5 on an average in the Universe.
- F.1. Methodology of arriving at 4% Baryonic matter :23% Dark Matter:73% Dark Energy ratio.
- Is this counter-intuitive model of our Universe made of dark matter and, blown apart by dark energy, correct?

To determine the escape velocity from our Universe we must satisfy the equation:

$\frac{1}{2} m v_{\text{esc}}^2 = GMm/R$ where R =radius of our Universe and M (this includes baryonic matter+ dark matter+ dark energy) = mass of our Universe; F.1

Eq.F.1 gives the escape velocity as

$$v_{\text{esc}} = \sqrt{(2GM/R)} \quad (\text{F2})$$

Since we have Flat Universe by observation:

Recession Velocity of the Observable Horizon (v_{rec}^*) = v_{esc} as given by Eq.G.2.

By Hubble's Law:

Recession Velocity of the Observable Horizon

$$= v_{\text{rec}}^* = R \times H_0 \quad (\text{F3})$$

where H_0 is the accepted value of Hubble Constant.

Equating Equation F.2 and Equation F.3 we get:

$$[(R \times H_0)]^2 = 2GM/R \quad \text{F.4}$$

Reshuffling the terms of Eq. F.4. we get the critical (matter+energy) density for our Flat Universe:

$$\Omega_{\text{crit}} = (3H_0^2)/8\pi G \quad \text{(F5)}$$

Substituting the numerical values of Hubble Constant and Gravitational Constant in Eq.G.5 we get the critical density as $9.38 \times 10^{-27} \text{Kg/m}^3$. This works out as 5.6 Hydrogen atoms per m^3 . This by Einstein mass-energy equivalence works out to be $8.43 \times 10^{-10} \text{Joules/m}^3$.

Let normalized actual (matter+energy) density $= \Omega_0$

$$\text{Then: } \Omega_{\text{act}}/\Omega_{\text{crit}} = \Omega_0 = 1 \text{ for Flat Universe (F6)}$$

Let normalized matter density be:

$$(\text{matter density})/\Omega_{\text{crit}} = \Omega_M \quad \text{(F7)}$$

Let normalized energy density be:

$$(\text{energy density})/\Omega_{\text{crit}} = \Omega_\Lambda \quad \text{(F8)}$$

Einstein had introduced the term $\Omega\Lambda$ as a cosmological constant in his Universe Equation to balance the gravitational collapse of the Universe and make it static.

Equating Eq.G.6 in terms of Eq.G.7 and Eq.G.8 we get:

$$\frac{\Omega_{\text{act}}}{\Omega_{\text{crit}}} = \Omega_0 = 1 = \Omega_M + \Omega_\Lambda \quad \text{(F9)}$$

Through the 42 type Ia Supernovae studies we get the following:

$$0.8\Omega_M - 0.6\Omega_\Lambda = -0.2 \pm 0.1 \quad \text{(F10)}$$

Using Eq.F.9 we solve Eq.F.10 we get:

$$\Omega_M = 0.28 \text{ hence } \Omega_\Lambda = 0.72.$$

Since Light Emitting Matter = Ordinary Baryonic Matter which contributes 0.01 to the normalized matter density of 0.28 therefore we can say that:

$$\text{Baryonic Matter: Dark Matter: Dark Energy} = 0.01:0.27:0.72 = 1\%: 27\%: 72\%.$$

By further refining the measurements and making the corrections we get:

$$\text{Baryonic Matter: Dark Matter: Dark Energy} = 4\%: 23\%: 73\%.$$

73% dark energy implies that eventually everything will become cold and hence dead therefore this is a very unlikely scenario and this one thing puts a big question mark on the Big Bang Theory.

What are the alternatives to the Big Bang?

Paul Steinhardt of Princeton University and Neil Turok of Cambridge University have proposed a new hypothesis "Endless Universe- beyond the Big Bang" by Random Press.

They propose that we live in a 10-D space and 1-D time. In this 10-D space there are two 3-D Universes which are connected to each other by 7th dimension. The 7th extra dimension is the gap between two parallel objects called Branes. These two Branes collide and create the Big-Bang without any singularity and without any gravitational waves radiation. Everything else will remain the same. We would still get the CMB radiation map as we are getting. There will still be continuous expansion leading to a cold Universe. But before they are dead the two universes collide and reset the clock. The cycle again begins. This goes on ad-infinitum.

Appendix G

ABELL 2029 consists of thousands of Galaxies enveloped in hot gas and dark matter. Total Mass of the dark matter is $100 \times 10^{12} \text{MO}$. X-Ray data shows that the dark matter increases smoothly all the way to the centre of the Galaxy Cluster. This distribution of dark matter matches the predictions of Cold Dark Matter. This cluster is at 1 bly from us. At the center there is an enormous, elliptical Galaxy acting as the anchor of the system.